

Article

Comparative population genomics reveals genetic basis underlying body size of domestic chickens

Ming-Shan Wang^{1,2}, Yong-Xia Huo^{1,3}, Yan Li⁴, Newton O. Otecko^{1,2}, Ling-Yan Su^{2,5}, Hai-Bo Xu^{1,2}, Shi-Fang Wu^{1,2}, Min-Sheng Peng^{1,2}, He-Qun Liu^{1,2}, Lin Zeng^{1,2}, David M. Irwin^{1,6,7}, Yong-Gang Yao^{2,5}, Dong-Dong Wu^{1,2,*}, and Ya-Ping Zhang^{1,2,4,*}

¹ State Key Laboratory of Genetic Resources and Evolution, Yunnan Laboratory of Molecular Biology of Domestic Animals, Kunming Institute of Zoology, Chinese Academy of Sciences, Kunming 650223, China

² Kunming College of Life Science, University of Chinese Academy of Sciences, Kunming 650204, China

³ College of Life Science, Anhui University, Hefei 230601, China

⁴ Laboratory for Conservation and Utilization of Bio-Resource, Yunnan University, Kunming 650091, China

⁵ Key Laboratory of Animal Models and Human Disease Mechanisms of the Chinese Academy of Sciences & Yunnan Province, Kunming Institute of Zoology, Kunming 650223, China

⁶ Department of Laboratory Medicine and Pathobiology, University of Toronto, Toronto, Ontario M5S 1A8, Canada

⁷ Banting and Best Diabetes Centre, University of Toronto, Toronto, Ontario M5G 2C4, Canada

* Correspondence to: Dong-Dong Wu, E-mail: wudongdong@mail.kiz.ac.cn; Ya-Ping Zhang, E-mail: zhangyp@mail.kiz.ac.cn

Body size is the most important economic trait for animal production and breeding. Several hundreds of loci have been reported to be associated with growth trait and body weight in chickens. The loci are mapped to large genomic regions due to the low density and limited number of genetic markers in previous studies. Herein, we employed comparative population genomics to identify genetic basis underlying the small body size of Yuanbao chicken (a famous ornamental chicken) based on 89 whole genomes. The most significant signal was mapped to the *BMP10* gene, whose expression was upregulated in the Yuanbao chicken. Overexpression of *BMP10* induced a significant decrease in body length by inhibiting angiogenic vessel development in zebrafish. In addition, three other loci on chromosomes 1, 2, and 24 were also identified to be potentially involved in the development of body size. Our results provide a paradigm shift in identification of novel loci controlling body size variation, availing a fast and efficient strategy. These loci, particularly *BMP10*, add insights into ongoing research of the evolution of body size under artificial selection and have important implications for future chicken breeding.

Keywords: body size, artificial selection, comparative population genomics, domestication

Introduction

Domestic animals are excellent biological models widely used in developmental biology, phenotypic evolution, and medical research studies. They have been developed as different breeds exhibiting remarkable differences in morphology, physiology, behavior, and adaptations (Darwin, 1868; Roots, 2007; Sutter et al., 2007; Menhenniott et al., 2013; Gou et al., 2014; Yoon et al., 2014; Wang et al., 2015a, 2016). As an economic character, body size of domestic animals is extremely important for humans and the development of human civilization. An amazing amount of body size variation is seen within domestic animals, which is much higher than that seen in their wild ancestors (Roots, 2007). In addition to breeders, both evolutionary and

developmental biologists are interested in discovering and characterizing the mechanisms that underlie the genetic control of variation in body size of domestic animals (Sutter et al., 2007; Makvandi-Nejad et al., 2012; Gou et al., 2014).

Domestic chickens are the most phenotypically variable bird (Darwin, 1868). For instance, bantam and cochin are amazing chicken breeds with adult body sizes at ~0.5 and ~5 kg, respectively, on the two extremes. As the farm animal with the widest distribution globally and raised in the largest number, domestic chickens have also been used in genetic and medical studies (Lawler, 2014). Genetic variants of specific traits, especially for body size, have been characterized, as they have major implications in both research and breeding (Sutter et al., 2007; Makvandi-Nejad et al., 2012; Gou et al., 2014). Several hundreds of quantitative trait loci (QTL) have been mapped and reported to be associated with growth and body weight of chickens (<http://www.animalgenome.org/cgi-bin/QTLdb/GG/index>).

Despite these achievements, most of these QTLs are mapped to large genomic regions due to the low resolution of low-density loci and limited number of microsatellite and SNP panel markers. Thus, only a limited number of causative loci have been identified. For example, some genes, including *IGF1*, *TBC1D1*, *FOXO1A*, *KPNA3*, *INTS6*, and *HNF4G*, have been associated with growth and body weight in chickens (Rubin et al., 2010; Gu et al., 2011; Elferink et al., 2012; Xie et al., 2012; Wang et al., 2015b). These studies were mostly based on commercial chickens with very limited variations, and most of the variants controlling body size could have likely been missed. Genome-wide association studies (GWAS) hold a promise for elucidating the quantitative genetic basis of this complex trait (Gu et al., 2011; Elferink et al., 2012; Xie et al., 2012; Wang et al., 2015b), although the difficulty of the methods and the high expense of collecting phenotypic data hamper its wide application. In addition, the great phenotypic diversity among the diverse breeds and their complicated demographic histories (Miao et al., 2013) have also impeded the study for genetic mechanisms underlying the variation of body size in chickens. Fortunately, next-generation genome sequencing data supplemented by comparative population genomics have revolutionized the fields of quantitative genetics and evolution, and thus have proved to be a powerful tool for interpreting the genetic underpinnings of complex traits in domestic animals, e.g. the head crest in the rock pigeon (Shapiro et al., 2013), cold adaptation of high latitude Chinese pigs (Ai et al., 2015), and adaptation to starch-rich foods by dogs (Axelsson et al., 2013).

Yuanbao chicken, a famous Chinese ornamental chicken breed, is known for its miniature body size, with adult male weight ~800 g and adult female ~500 g. It has a long breeding history that can be traced back to the Tang dynasty (Supplementary Figure S1). Both the small body size that makes it easily handled in the palm and the appearance similar to 'Yuanbao', a metallic ingot used in ancient China as money, made Yuanbao chicken be treated as a symbol of wealth at hand in ancient times (Supplementary Figure S1). To date, Yuanbao chicken is indisputably one of the most esteemed chicken breeds in China. Here, we employed comparative population genomics to study the genetic basis underlying the small body size of Yuanbao chicken. We identified four novel loci that potentially control the variation in body size of domestic chickens.

Results

Analyses of 89 chicken genomes identify >20 million SNPs

In this study, 89 genomes were obtained representing 7 Red Junglefowls, 24 Yuanbao chickens (Supplementary Figure S1), and 58 other domestic chickens, with ~12.2× sequence coverage for each individual (Supplementary Figure S2 and Table S1). Comparisons among the genome sequences identified a total of 21286312 SNPs, with 51.8% of them mapping to intergenic regions, 42.6% to intronic regions, and only a small proportion (1.5%) mapping to exonic regions of the genome (Supplementary Table S2). Functional annotation of the SNPs assigned to protein-

coding regions identified 101999 SNPs that produce non-synonymous amino acid substitutions and 226713 SNPs that were synonymous, with 704 genes having SNPs that cause gain or loss of a stop codon (Supplementary Table S3). Further comparisons indicated that 88% and 90% of the SNPs used in the 60 K Illumina BeadChip genotyping array and the 600 K Affymetrix® Axiom® HD genotyping array, respectively, were contained in our new dataset. Our dataset of SNPs is much larger than those available in the chicken SNP database: 14353694 and 8670333 of our SNPs were not reported in BUILD 138 and BUILD 145 of the chicken dbSNP databases (ftp://ftp.ncbi.nih.gov/snp/organisms/chicken_9031), respectively. These novel SNPs potentially supplement the catalog of chicken variants.

Compared with other birds, Yuanbao chicken showed a lower level of nucleotide diversity (mean value: 4.56E-03) (Supplementary Figure S3). A phylogenetic tree of all individuals was constructed using weighted neighbour-joining method (Bruno et al., 2000), which revealed that Yuanbao chicken formed a relatively homogeneous ancestral cluster (Figure 1A). Principle component analysis (PCA) (Figure 1B), admixture (Supplementary Figure S4), and haplotype-based structure analyses (Supplementary Figure S5) indicated that several Yuanbao chickens had mixed ancestry with other chicken breeds.

Comparative population genomics as a strategy to identify loci controlling body size variation in chickens

Comparative analysis of population variants is a powerful tool that has enabled successful investigation into genetic mechanisms underlying complex traits (Axelsson et al., 2013; Kamberov et al., 2013; Shapiro et al., 2013; Ai et al., 2015; Lamichhane et al., 2015). Since Yuanbao chicken has a remarkably smaller body size compared to the average body size of chickens, comparative genome analysis of Yuanbao and other chickens would be an effective strategy to identify the genetic basis underlying the variation in body size among chickens. Here, we employed F_{ST} and LSBL (Shriver et al., 2004) to evaluate the population differentiation of Yuanbao chicken from other chickens (Figure 1C and D). First, a sliding window analysis was performed, with 50 kb window size and 25 kb step size, identifying 268 and 275 genes from the empirical data with F_{ST} and LSBL, respectively, as candidates based on the outlier approach (99th percentile cutoff). Functional enrichment analysis of these candidate genes did not reveal any pathway specifically associated with the development of body size (Supplementary Tables S4 and S5). By combining the signals of F_{ST} and LSBL, we identified four regions of the genome (chr22:0.25Mb–0.33Mb, chr1:147.55Mb–147.82Mb, chr2:57.05Mb–57.22Mb, and chr24:6.1Mb–6.3Mb) that exhibited extreme population differentiation, likely as the result of artificial selection.

Analysis of chr22:0.25Mb–0.33Mb shows BMP10 potentially controlling the body size of Yuanbao chicken

The genomic region chr22:0.25Mb–0.33Mb stands out as the most extremely candidate selective sweep with the highest level of population differentiation (Figure 1C). There are three genes *GKN1*, *GKN2*, and *BMP10* located in this region (Figure 2A).

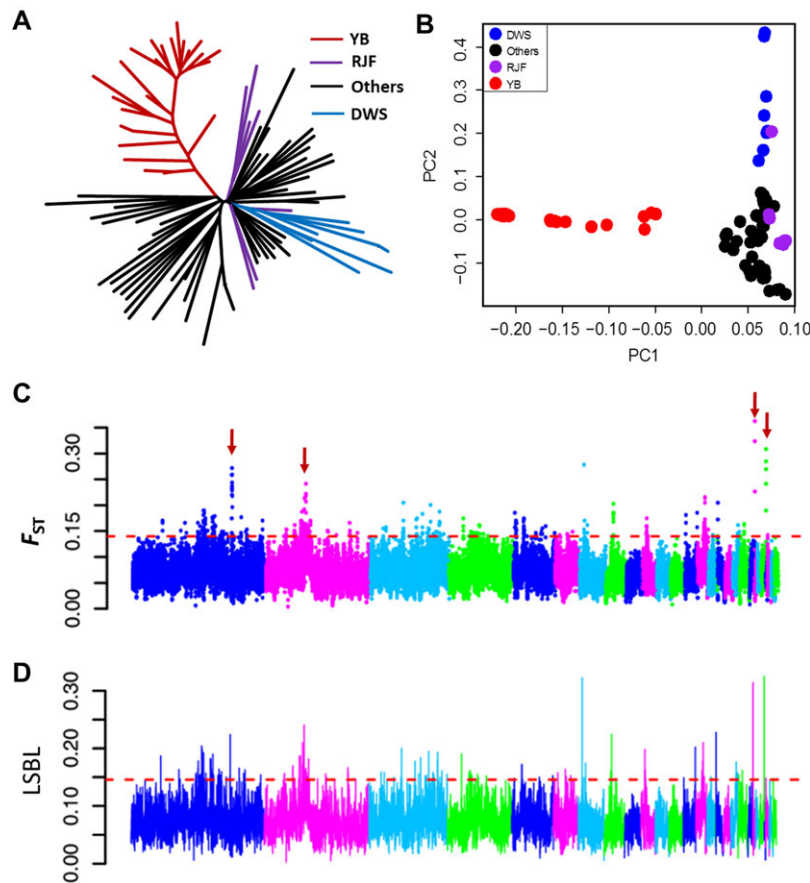


Figure 1 Phylogenetic and positive selection analyses. **(A)** Neighbour-joining tree of 89 chicken genomes. **(B)** PCA. **(C and D)** Genomic landscape of population differentiation by F_{ST} **(C)** and LSBL **(D)**. Four significant clusters are marked and presented. YB, Yuanbao chicken; RJF, Red Junglefowl; DWS, Daweishan chicken.

GKN1 and *GKN2* are paralogues abundantly and uniquely expressed in the stomach (Menheniott et al., 2013). Both genes have documented functional importance in maintaining integrity and normal function of gastric mucosa, and their anomaly is associated with gastric cancer (Kim et al., 2014; Yoon et al., 2014). In Yuanbao and other chickens, both *GKN1* and *GKN2* exhibited no or extremely low expression levels in the heat, kidney, spleen, muscle, liver, and lung (Supplementary Figure S6).

BMP10, a member of the transforming growth factor β (TGF β) family, showed consistently higher values in F_{ST} and LSBL analyses and high differences in allele frequencies (Figure 2A–C). A haplotype comparison analysis revealed a consistent differentiation of *BMP10* for Yuanbao chicken from other chickens (Figure 2D). Until now, a role of *BMP10* in body size has not been reported in chickens. In addition, no QTL associated with body size in chickens was mapped to this genomic region.

Further investigation showed that *BMP10* had a high expression in the heart (Supplementary Figure S7), and the expression level was significantly upregulated in Yuanbao chicken compared to other chickens (Figure 3A). Phylogenetic network analysis based on the Sanger resequencing verified data also supported the conclusion that the promoter region of *BMP10*

has become highly differentiated in Yuanbao chicken compared to other chickens (Figure 3B). To examine promoter activity, we performed luciferase reporter gene assays with *BMP10* promoter sequence from Yuanbao chicken and the reference sequence. Consistently, we observed an increased reporter activity driven by the *BMP10* promoter of Yuanbao chicken compared to the reference promoter (Figure 3C and D). Next, based on our phylogenetic network, we identified 21 SNPs that were located upstream of *BMP10* and showed high differentiation between Yuanbao and other chickens. These SNPs were further examined to investigate differences in DNA–protein interactions by electrophoretic mobility shift assays (EMSA) with nuclear extracts from chicken hearts. Probes for five of these SNPs showed differences in gel shift between Yuanbao and other chickens (Figure 3E and Supplementary Figure S8). Mutations in Yuanbao chicken at chr22:274606(T→C) and chr22:274758 (C→deletion) led to decrease or loss of interactions between DNA and protein. On the other hand, mutations in Yuanbao chicken at chr22:274670(A→G), chr22:276118(A→G), and chr22:276140 (C→T) increased the DNA–protein interaction. From these observations, we inferred that the differences in protein binding, due to the underlying SNPs, likely contribute to the upregulation of

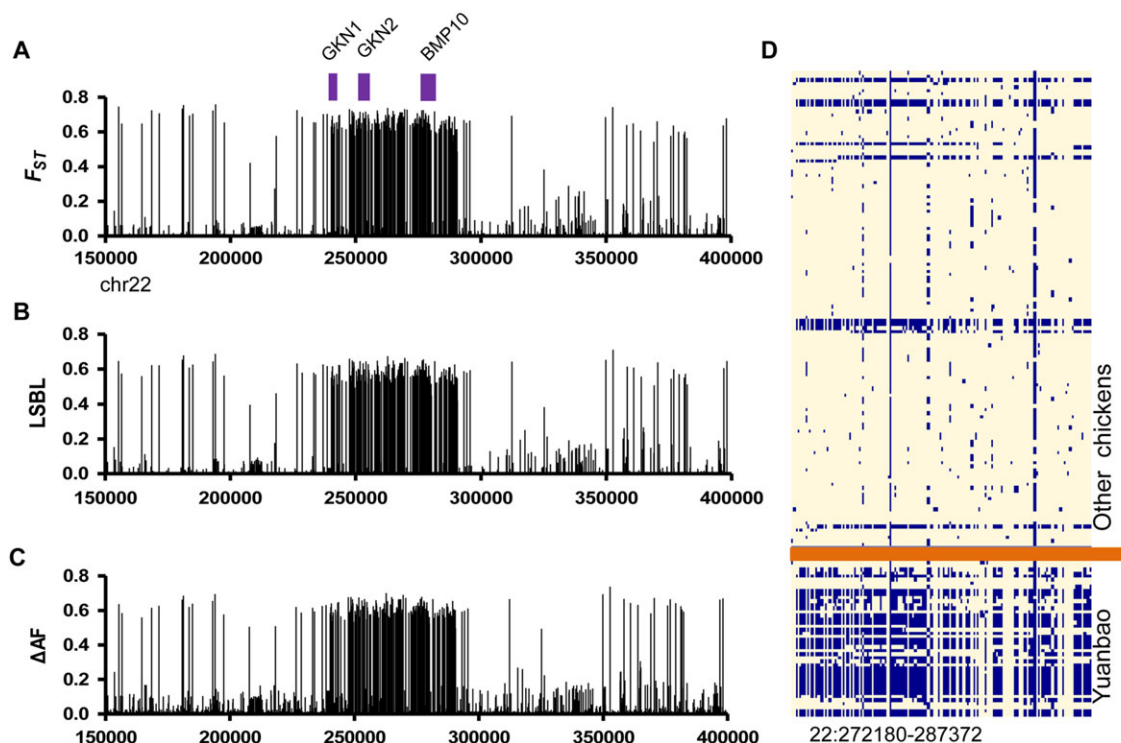


Figure 2 Population differentiation in chr22:0.25 Mb–0.33 Mb between Yuanbao and other chickens. (A–C) Landscape of F_{ST} (A), LSBL (B), and ΔAF (C). (D) Haplotype comparison between Yuanbao and other chickens. Alternative alleles are labelled in blue.

BMP10 expression in the heart of Yuanbao chicken (Figure 3A). We further genotyped one SNP within this strong linkage region, which showed a significant association with body weight (Figure 3F, $P = 3.249E-18$). The SNP could explain 22.41% of the overall weight variance in five chicken lines, i.e. Jiningbairi chicken, Luhua chicken, bantam, Yuanbao chicken, and ornamental chicken.

BMP10 overexpression inhibits angiogenesis and induces short body length in zebrafish

Overexpression of *BMP10* induced a decrease in body weight in mice (Chen et al., 2006). To examine whether it is a conserved function of *BMP10* to control body size in vertebrates, we performed an overexpression assay of wild-type *BMP10* in zebrafish. Fertilized one-cell zebrafish embryos from the *fli1a-EGFP* transgenic line were injected with 200 pg wild-type zebrafish *BMP10* mRNA per embryo respectively. Overexpression of *BMP10* in zebrafish resulted in a decreased body length and a curved body axis compared to uninjected control embryos (Figure 4 and Supplementary Figure S9). These results affirm that *BMP10* has an important role in determining body size. Angiogenesis is a normal and vital process in growth and development (Folkman and Shing, 1992). To study the phenotypic consequence of *BMP10* overexpression on angiogenesis in zebrafish, we anesthetized transgenic embryos with 0.016% tricaine methanesulfonate (MS-222) and counted the number of complete intersegmental vessels (ISVs) at 32 h post-fertilization (hpf). Zebrafish with overexpression of *BMP10* showed a larger

number of incomplete ISVs and only occasional sprouts of dorsal aorta (DA) compared with the control zebrafish (Figure 5 and Supplementary Figure S10). These results indicate that overexpression of *BMP10* inhibits angiogenic vessel growth in zebrafish, which would inhibit growth and result in a shorter body. All these data suggest that upregulation of *BMP10* likely contributes to a smaller body size of Yuanbao chicken.

Genes at chr1:147.55Mb–147.82Mb, chr2:57.05Mb–57.22Mb, and chr24:6.17Mb–6.25Mb are potentially involved in the development of body size

Chr1:147.55Mb–147.82Mb, harbouring a cluster of selective sweep SNPs, demonstrates significantly higher levels of population differentiation as revealed by F_{ST} (Figure 1C) and LSBL (Figure 1D). No annotated gene is located in this region. However, this region is located within a previously reported QTL associated with ‘Body weight’ and ‘Growth’ (Carlborg et al., 2003; Gu et al., 2011). The gene *GPC5*, which plays a role in the control of cell division and growth regulation (Yang et al., 2013), is found adjacent to this mapped location. RNA-seq analysis showed that expression of *GPC5* was downregulated in the heart of Yuanbao chicken (Supplementary Figure S11A, $P < 0.05$).

Similar to that in chr1:147.55Mb–147.82Mb, no protein-coding gene is located in the chr2:57.05Mb–57.22Mb genomic region, although it also displayed strong signals of selection with high levels of population differentiation as revealed by F_{ST} (Figure 1C) and LSBL (Figure 1D). QTL mapping has shown that this region is strongly associated with ‘Body weight’ and

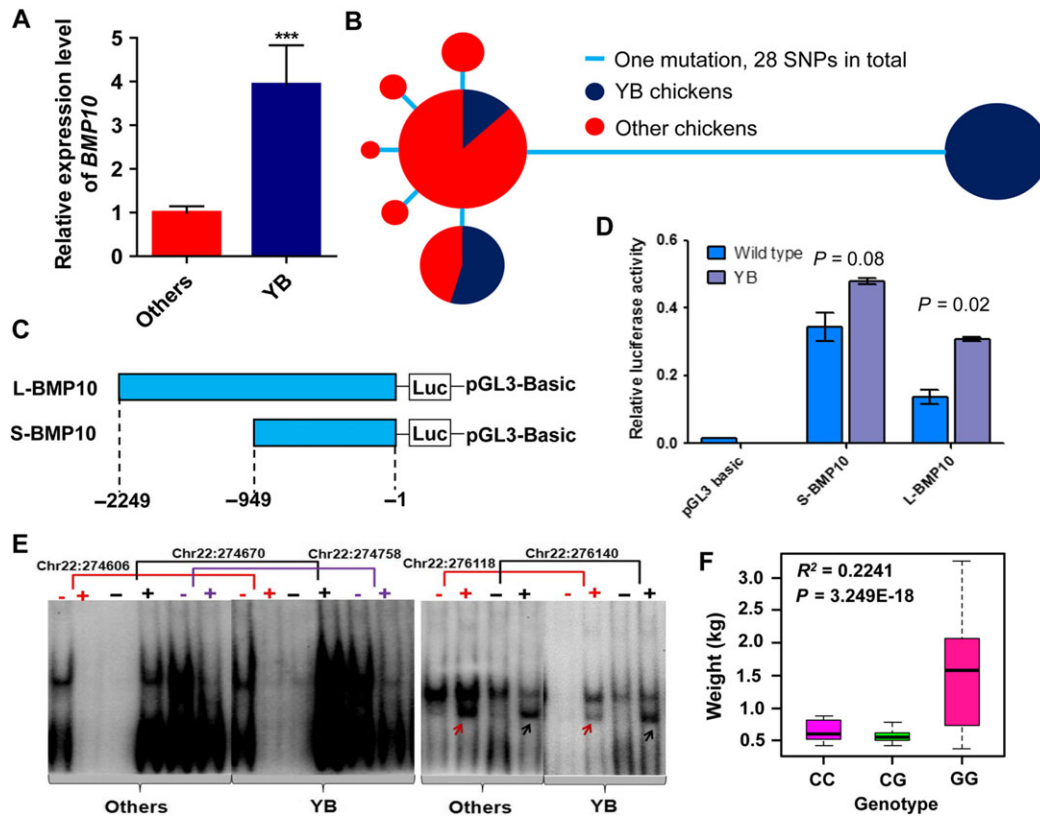


Figure 3 Expression and association analysis of the gene *BMP10*. (A) Comparison of the expression of *BMP10* in heart tissue between YB and other chickens. (B) Median joining network of the *BMP10* promoter haplotypes. (C) Schematic structure of luciferase reporter plasmids with different lengths. (D) Comparison of luciferase activity of the promoters between YB and other chickens. (E) Five SNPs present differential mobility by EMSA. '+' and '-' refer to probes with the mutated YB allele and reference allele, respectively. (F) Association analysis of *BMP10* and weight. G is the reference allele. Statistical significance is measured by Student's *t*-test. Error bar represents SEM. YB, Yuanbao chicken.

'Growth rate' in chickens (Carlborg et al., 2003; Siwek et al., 2004; Tercic et al., 2009). Chr2:57.05Mb–57.22Mb is upstream of the gene spalt-like transcription factor 3 (*SALL3*), a transcription factor that plays a fundamental role in animal development (de Celis and Barrio, 2008). We observed an upregulated expression of *SALL3* in kidneys of Yuanbao chicken compared to village domestic chicken ($P = 0.0208$) and Red Junglefowl ($P = 0.24795$) (Supplementary Figure S11B).

The forth mapped region chr24:6.17Mb–6.25Mb contains 13 protein-coding genes (Supplementary Table S6). There is no QTL associated with body weight or growth rate in this region. These 13 genes are involved in various biological processes (Supplementary Table S6). For example, *BCO2* is associated with skin colour in chickens (Eriksson et al., 2008), while *DIXDC1* and *CRYAB* are involved in nervous system (Ousman et al., 2007; Kivimae et al., 2011). *HSPB2*, a heat shock protein (HSPs) gene, is highly expressed in the heart and skeletal muscle, which is essential in maintaining muscle cell integrity in some mouse skeletal muscles. Knockdown of *HSPB2* results in degeneration of skeletal muscle in mice (Brady et al., 2001). In our study, the expression of *HSPB2* was downregulated in the muscle of Yuanbao chicken compared to village domestic

chicken ($P = 0.0682$) and Red Junglefowl ($P = 0.06205$) (Supplementary Figure S12).

Discussion

Chickens are of integral dietary importance (e.g. egg and meat) in many communities globally. They are also raised for other purposes like biological research and entertainment. For the source of food and economic income, breeders have made great effort to develop chickens with a large body size and rapid growth rate for meat production (Lawler, 2014). Our study reports four loci that potentially control body size, providing important information and candidate genetic markers for chicken breeding. Our study also provides a strategy with comparative population genomics to identify candidate genes/variants accounting for the variation in the body size of chickens. This strategy is much more cost-effective and timesaving than previous methods such as QTL mapping and GWAS analysis.

A great variation in body size has been observed in several domesticated animals, including dogs, pigs, and chickens (Roots, 2007). Body size is not only an important commercial trait for food production, but also a key topic for evolutionary and developmental biology studies (Sutter et al., 2007;

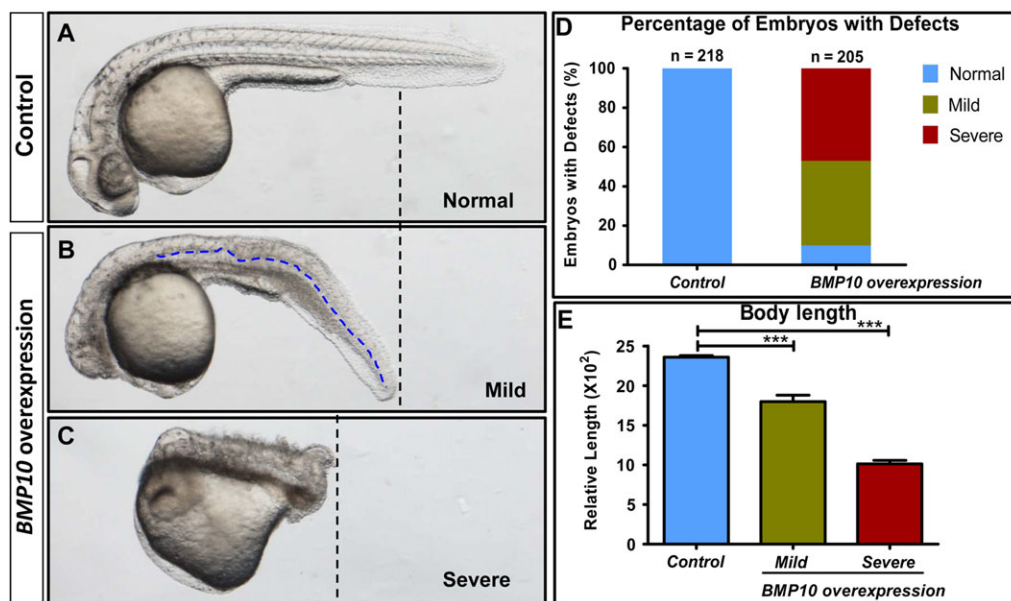


Figure 4 Overexpression of *BMP10* induces developmental defects in Zebrafish. (A–C) Gross morphology at 32 hpf. Compared with un-injected wild-type control embryos, embryos with wild-type zebrafish *BMP10* overexpression exhibited a decreased body length (indicated by the black dotted line) and a curved body axis (indicated by the blue dotted line). See Supplementary Figure S9 for more samples. (D and E) Bar graphs show that the *BMP10* overexpression caused higher percentage of embryos with developmental defects and shorter body length.

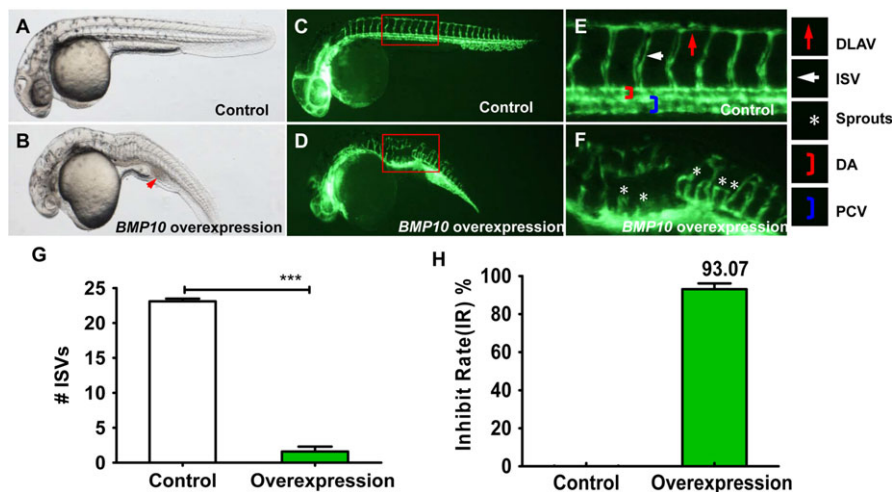


Figure 5 Overexpression of *BMP10* inhibits angiogenesis in Zebrafish. (A–F) Representative bright field and fluorescent images of zebrafish embryos at 32 hpf. Red arrow indicates haemorrhage in the tail (B). (C–H) Compared to wild-type control, the fish injected with wild-type zebrafish *BMP10* mRNA (200 pg) less incomplete ISVs and occasional sprouts (marked with asterisk) of the dorsal aorta. The regions boxed in red are shown in higher magnification to the right. DLAV, dorsal longitudinal anastomotic vessels; ISV, intersegmental vessels; DA, dorsal aorta; PCV, posterior cardinal vein.

Makvandi-Nejad et al., 2012; Rubin et al., 2012; Rimbault et al., 2013; Qanbari et al., 2014). The investigation in genes/genetic variants controlling variation in body size has attracted attentions from animal breeders, evolutionary and developmental biologists, and even medical scientists (Sutter et al., 2007; Makvandi-Nejad et al., 2012; Gou et al., 2014).

Body size, typical of many complex traits, is commonly believed to be influenced by many genes involved in similar

functional pathways (Devlin et al., 2009). For example, in a study of humans, 97 loci associated with body mass index (BMI) were identified, yet these loci only account for ~2.7% of BMI variation (Locke et al., 2015). In stark contrast, very few genes have been reported to be involved in the evolution of body size in domestic animals. For example, derived variants at six genes explain nearly half of the size reduction seen in some dog breeds (Rimbault et al., 2013). In horses, a similar pattern

was reported, where four loci explained 83% of the variation in body size (Makvandi-Nejad et al., 2012). Here, we also found that *BMP10* could explain 22.41% of body size variation in five chicken lines, including Jiningbairi chicken, Luhua chicken, bantam, Yuanbao chicken, and ornamental chicken. These contrasting patterns between humans and domestic animals are likely explained by the differences in natural vs. artificial selection.

In assessing the genetic basis underlying the small body size of Yuanbao chicken, we identified several genomic regions associated with morphogenic genes. A non-genic region was identified on chromosome 1 (chr1:147.55Mb–147.82Mb). This sequence is upstream of the protein-coding gene *GPC5* and showed evidence of positive selection, whose expression was downregulated in the heart of Yuanbao chicken. The human *GPC5* locus has been reported to be associated with height (Lango Allen et al., 2015). A GWAS based on the Illumina 60 K Chicken SNP Beadchip also found evidence for a potential association of *GPC5* with body weight in domestic chickens (Sewalem et al., 2002; Carlborg et al., 2004; Gu et al., 2011). Similarly, no protein-coding gene was found in the selected region of chromosome 2 (chr2:57.05Mb–57.22Mb), which is located upstream of another gene involved in development, *SALL3* (Parrish et al., 2004; Kojima et al., 2013). The expression of *SALL3* was upregulated in kidneys of Yuanbao chicken. Whether *SALL3* has a function in controlling body size is unclear. But *SALL3* protein directly binds to DNA methyltransferase 3 alpha (DNMT3A) and reduces DNMT3A-mediated CpG island methylation (Shikauchi et al., 2009). *DNMT3A* is necessary for the control of body weight and energy homeostasis (Kohno et al., 2014), and is associated with height in humans (Gudbjartsson et al., 2008). In addition, expression of *SALL3* can be induced by *BMP4* (Shikauchi et al., 2009), a bone morphogenetic protein (BMP) that plays an important role in the development of the skeletal system. Mouse mutants with double-null *Sall1/Sall3* exhibited malformation in limb morphogenesis (Kawakami et al., 2009). In a selective sweep region in chromosome 24 (chr24:6.17Mb–6.25Mb), there were 13 protein-coding genes with diverse biological functions. *HSPB2*, a gene essential for skeletal muscle development, was downregulated in Yuanbao chicken, likely showing an association with the unique growth properties of Yuanbao chicken. Three protein-coding genes *GKN1*, *GKN2*, and *BMP10* were found in the selected region of chromosome 22 (chr22:0.25Mb–0.33Mb). Both *GKN1* and *GKN2* are highly and uniquely expressed in the stomach, with important roles in maintaining its normal function. *BMP10* is specifically expressed in the heart and plays a crucial role in regulating the development of the heart in mice (Neuhaus et al., 1999). *BMP10*-deficient mice survived through E10.0–E10.5 and then died due to severely impaired cardiac development and function (Chen et al., 2004). Overexpression of *BMP10* in mice leads to myocardial overgrowth and hypertrabeculation in embryos (Pashmforoush et al., 2004). Transgenic mice with postnatal overexpression of *BMP10* in the myocardium display a 50% deduction in the heart size and a reduction in body weight

and size at the age of 1 month (Chen et al., 2006). *BMP10* is also reported to have a role in inducing apoptosis, proliferation, and growth of cells (Kawakami et al., 2009; Kim et al., 2014). For example, *BMP10* expression was observed to be decreased or absent in prostate tumours, and forced *BMP10* overexpression decreased *in vitro* growth, cell matrix adhesion, invasion, and migration of prostate cancer cells (Kawakami et al., 2009). Further examination showed that *BMP10* expression was upregulated in the heart of Yuanbao chicken, probably as a result of five potential mutations upstream of *BMP10* that likely increased the promoter activity. Similar to that in mice (Chen et al., 2006), an overexpression of *BMP10* induced a decrease in body length in zebrafish, implying a conserved function of *BMP10* in controlling body size in vertebrates. The four loci identified in our study, with high population differentiation between Yuanbao and other chickens, potentially influence gene expression rather than protein-coding sequence. This potentially supports a model that changes of gene expression contribute significantly to the evolution of body size, a view consistent with the hypothesis that changes in gene expression are particularly important in morphological evolution (Carroll, 2008; Young et al., 2015).

There are still some limitations in our study. First, we supposed that five mutations could have likely changed the promoter activity of *BMP10* leading to higher expression of *BMP10* in Yuanbao chicken. Two mutations chr22:274606(T→C) and chr22:274758(C→deletion) lead to decrease or loss of DNA–protein interactions, while the other three mutations chr22:274670(A→G), chr22:276118(A→G), and chr22:276140(C→T) increased DNA–protein interactions. Our study could not single out which proteins were involved in these interactions, neither whether all or only some of these sites work together to activate the promoter of *BMP10*. In addition, some miniature domestic chicken breeds have similar body size as Yuanbao chicken, but we only include Yuanbao chicken as a small body-sized chicken line in our study. Furthermore, the chromosomal region containing *BMP10* gene in Daweishan chicken was in the same wild-type state as in Red Junglefowl and other domestic chicken lines. Hence, we cannot definitely conclude that *BMP10* has a common consequence in other domestic chicken lines, especially due to the complex origin and demographic history of domestic chickens (Miao et al., 2013). Broader sampling to include more chicken breeds with small body size and additional work will help address these issues in the future.

Materials and methods

Animal experimental ethics

All animal experimental procedures were performed according to the guidelines approved by the Ethics Committee of Kunming Institute of Zoology.

Sampling and genomic data collection

Up to 42 genomes, including 24 Yuanbao chickens (YB), 8 Daweishan chickens (DWS, a semi-domestic and miniature breed), 1 Red Junglefowl (RJF), 6 Guangzhou local chickens, and

3 Yunnan local chickens were sequenced in this study (Supplementary Table S1). DNA was extracted using the phenol-chloroform extraction method and the quality was measured by electrophoresis and on a NanoDrop spectrophotometer 2000. Only high-quality DNA was used for the construction of genome sequencing libraries according to the Illumina standard genome library preparation pipeline. Sequencing was performed on an Illumina HiSeq 2000 platform with a read length of 101 bp. Genomes for 33 chickens from our previous study (Wang et al., 2015a), 2 chickens from the study by Fan et al. (2013), and 12 chickens from the study by Yi et al. (2014) were integrated into our study (Supplementary Table S1). Overall, 89 genomes for 7 Red Junglefowls and 82 domestic chickens were obtained.

Genomic sequence alignment, SNP calling and annotation

Raw sequence reads were filtered by removing adaptors and low-quality bases using cutadapt and Btrim software (Kong, 2011). Qualified reads were aligned onto the chicken reference genome (Galgal4) using BWA-MEM with default settings except the '-t 8 -M' options (<https://github.com/lh3/bwa>). A series of post-processes were then employed to process the alignment BAM format file, including sorting, duplicates marking, local realignment, and base quality recalibration, which were carried out using the SortSam and MarkDuplicates functions in the Picards (picard-tools-1.56, <http://picard.sourceforge.net>) package, and RealignerTargetCreator, IndelRealigner, and BaseRecalibrator tools in the Genome Analysis Toolkit (GenomeAnalysisTK-2.6-4, GATK) (McKenna et al., 2010). SNPs and indels were called and filtered using UnifiedGenotyper and VariantFiltration command in GATK. Loci with RMS mapping quality <25 and genotype quality <40, for which reads with zero mapping quality constitute >10% of all reads at this site were removed. Loci with >2 alleles and within clusters (>3 SNPs in a 10-bp window) were removed. All SNPs were assigned to specific genomic regions and genes using ANNOVAR based on the ENSEMBL chicken annotations (Wang et al., 2010). Missing SNPs with <10% frequency were imputed, and haplotypes for each chromosome were deduced by BEAGLE (BEAGLE 3.3.2.) (Browning and Browning, 2007).

Population variation and population genetic analyses

Genome-wide genetic diversity (π) was calculated for Yuanbao chicken, Red Junglefowl, Daweishan chicken, and other chicken groups using VCFtools (Danecek et al., 2011) using a 50-kb sliding window with 25-kb stepwise increments. Several methods were applied to infer the population structure of Yuanbao chicken. First, we constructed a neighbour-joining tree using the software PHYLIP (Bruno et al., 2000) based on the pairwise distance matrix derived from the simple matching distance for all SNP sites. The tree was viewed using MEGA5 (Tamura et al., 2011). Second, to minimize the effects of SNPs contributed by regions of extensive strong linkage disequilibrium (LD), we pruned the SNPs according to the observed sample correlation coefficients using PLINK (Purcell et al., 2007) with the parameter '--indep 100 50 0.1', and PCA was performed using GCTA (Yang et al., 2011). Third, admixture analysis was

performed to view the population structure by using ADMIXTURE (Alexander et al., 2009) with an ancestor population size ranging from 2 to 5, based on the pruned data. Fourth, we used a haplotype-based approach, ChromoPainter and fineSTRUCTURE, to infer population structure (Lawson et al., 2012).

Genome-wide selective sweep analysis

We employed three tests to investigate the genomic regions harbouring footprints of positive selection in Yuanbao chicken. F_{ST} values for each SNP were estimated between Yuanbao and other chickens as described elsewhere (Akey et al., 2002). LSBL statistics were calculated for each SNP based on the F_{ST} values between the three groups (Shriver et al., 2004). Here we defined Yuanbao chicken as group A, Red Junglefowl and Daweishan chicken as Group B since Daweishan chicken possesses features similar to Red Junglefowl (i.e. appearance, habits, and characters). Other domestic chicken lines were assigned group C. LSBL statistics for each variant was calculated using the formula: $LSBL = (F_{ST(AB)} + F_{ST(AC)} - F_{ST(BC)})/2$. Sliding window analysis was performed for F_{ST} and LSBL in each 50-kb window with 25-kb stepwise increments. In addition, we computed the absolute allele frequency difference (ΔAF) per SNP between Yuanbao and other chickens to confirm the signal of positive selection (Carneiro et al., 2014). Deduced candidate selective sweeps detected by above methods were annotated using the Variant Effect Predictor available at <http://asia.ensembl.org/info/docs/tools/index.html>. Functional enrichments of protein-coding genes including Gene Ontology (GO) categories, KEGG pathway, and Human Phenotype Ontologies (HPO) were analyzed using g:Profiler (Reimand et al., 2011).

SNP verification and network construction

Sanger resequencing on an Applied Biosystems ABI 3730XL Genetic Analyzer, was used to verify SNPs in the region upstream and in the first exon of the *BMP10* gene. A total of 54 chickens, including Yuanbao chicken and local indigenous chickens, were used for confirmation. Primers used for amplification and sequencing are listed in Supplementary Table S7. Haplotypes were phased using PHASE program (Stephens and Donnelly, 2003). A median-joining network was constructed using Network (Bandelt et al., 1999).

Genotyping and association analysis

To further define how variation at *BMP10* contributes to the body size, we genotyped one SNP (chr22:276457, G/C) in overall 301 chickens from five chicken lines (Jiningbairi chicken, Luhua chicken, bantam, Yuanbao chicken, and ornamental chicken) with available body weight information using Sanger resequencing method. The proportion of weight variation explained was estimated using PLINK with the linear model (Purcell et al., 2007).

RNA extraction and real-time quantitative PCR assay

Total RNA was isolated from heart, liver, spleen, lung, muscle, kidney, and brain tissues of adult chickens using TRNzol-A+ Reagent

(TIANGEN) and purified using RNeasy Micro Kit (QIAGEN). The concentration and integrity of the RNA was measured using electrophoresis and NanoDrop spectrophotometer 2000. Total RNA (~2 µg) was used to synthesize single-strand cDNA using the PrimeScript RT-PCR Kit in a final volume of 25 µl according to the manufacturer's instructions. Relative mRNA expression levels of *BMP10* in the chicken heart were measured using real-time quantitative PCR (qPCR) with the relative standard curve method and normalization to the housekeeping gene *GAPDH*. Primer pairs used for *BMP10* are listed in Supplementary Table S8. qPCR was performed on the iQ2 system platform (BioRad Laboratories, Hercules) with SYBR® Premix Ex Taq™ II Kit. Student's *t*-test was used to measure the statistical significance.

RNA-seq analysis

For RNA-seq analysis, we included 47 transcriptomes from lung, heart, muscle, spleen, liver, and kidney tissues of Yuanbao chicken, village domestic chicken, and Red Junglefowl, which were generated using Hiseq platform in one of our projects (see Supplementary Table S9). Firstly, poor-quality reads were filtered out using Trimmomatic (Bolger et al., 2014), with parameters set to 'LEADING:5 TRAILING:5 SLIDINGWINDOW:4:10 MINLEN:50'. Secondly, clean reads were aligned onto chicken reference genome (Galgal4) using HISAT2 (Kim et al., 2015) with parameters set to '-sp 1000,1000 --k 20 --no-unal --dta --dta-cufflinks --no-discordant' StringTie (Pertea et al., 2015). Cuffcompare (Trapnell et al., 2012) were then used to assemble new transcripts and compare the assembled transcripts with the annotated reference transcripts to generate a new-merged GTF annotation file. Cuffdiff (Trapnell et al., 2012) was used to measure the significance of the gene expression difference for each tissue between Red Junglefowl and Yuanbao chicken, as well as between village domestic chicken and Yuanbao chicken. *P*-value was calculated based on the Poisson fragment dispersion model (default by cuffdiff program) (Trapnell et al., 2012).

Luciferase reporter analysis

To infer whether the highly differentiated SNPs in the upstream of *BMP10* in Yuanbao chicken increased the *BMP10* promoter activity, we performed a luciferase reporter assay. Two upstream fragments of the *BMP10* gene, a long 2449-bp fragment (L-BMP10, chr22:274094–276542) and a short 949-bp fragment (S-BMP10, chr22:275594–276542), respectively, were generated by PCR and cloned into the pGL3 Basic vector (Promega). *KpnI* and *XhoI* enzyme sites were used to construct the vectors. Human embryonic kidney 293T cells (HEK 293T) plated in 24 wells were transfected at 60%–70% confluency with the pGL3 reporter plasmids and 80 ng of pRL-TK Renilla luciferase construct in each well using Lipofectamine™ 2000 (Invitrogen). Luciferase activity was measured at 24 h after transfection using the GloMax® 96 Microplate Luminometer (Promega). Ratios of Firefly luminescence/Renilla luminescence were calculated with the Basic vector as the reference. Three technical replicates

were performed. Student's *t*-test was used to measure the statistical significance between Yuanbao and other chickens.

Electrophoretic mobility shift assays

A total of 21 SNPs within 2249-bp upstream region from start site of the *BMP10* gene, which were also verified by Sanger sequencing, were selected for a functional assay using EMSA to reveal potential differences in DNA–protein interactions. A total of 20 pairs of 5'Biotin-labelled probes (mutations at chr22:276330 (T→C) and chr22:276331(G→A) shared one probe) were synthesized (Integrated DNA Technologies). Heart tissues from 4 chickens (including one Yuanbao chicken and three Chinese local domestic chickens) were collected after the chickens were sacrificed and stored at –70°C until further analysis. Nuclear extracts were prepared from the heart tissue using NucBuster Protein Extraction Kit (Viagene Biotech). The nuclear extracts (2.1 µg) were added to the binding reaction and then preincubated for 20 min on ice. For the competition reactions, 20 pmol of unlabelled double-strand oligos were added to the reactions. After preincubation, 20 fmol of the biotinylated oligos were added to the reactions and incubated for 20 min at room temperature. DNA–protein complexes were separated by electrophoresis on 6.5% non-denaturing polyacrylamide gel at 120 V for 90 min in 0.5× TBE running buffer. Separated complexes were transferred to binding-membrane (Viagene Biotech) at 390 mA for 40 min in cold 0.5× TBE. DNA–protein complexes were crosslinked using Stratalinker UV Crosslinker, and biotinylated probes were detected using Lighten® HRP-B Substrate Solution A and B (Viagene Biotech).

Zebrafish care and maintenance

Adult zebrafish were maintained at 28.5°C on a 14-h light/10-h dark cycle (Westerfield, 1993). Four to five pairs of zebrafish were set up for natural mating for every cross. On average, 100–200 embryos were generated. Embryos were maintained at 28.5°C in fish water (0.2% instant ocean salt in deionized water). Embryos were washed and staged according to Kimmel et al. (1995). The establishment and characterization of the *fli1a-EGFP* transgenic line has been described elsewhere (Lawson and Weinstein, 2002). The zebrafish facility at the Shanghai Biomodel Organism Science & Technology Development Co., Ltd is accredited by the Association for Assessment and Accreditation of Laboratory Animal Care (AAALAC) International.

Zebrafish microinjection

For the overexpression assay, fertilized one-cell embryos were injected with 200 pg wild-type zebrafish *BMP10* mRNA per embryo.

Zebrafish angiogenesis studies

To evaluate blood vessel formation in zebrafish, fertilized one-cell *fli1a-EGFP* transgenic embryos were injected with 200 pg wild-type *BMP10* mRNA per embryo. At 32 hpf, embryos were anesthetized with 0.016% MS-222 (Sigma-Aldrich), and the number of complete ISVs, which connect the DA to the

DLAV, was counted. The anti-angiogenesis effect was determined using the following formula:

$$\% \text{ inhibition} = \left(1 - \frac{\text{ISV amount of experiment group}}{\text{ISV amount of wild type control}} \right) \times 100 \quad (\text{a})$$

Image acquisition

Embryos and larvae were examined with a Nikon SMZ 1500 Fluorescence microscope and subsequently photographed with digital cameras. A subset of images were adjusted for levels of brightness, contrast, hue, and saturation with Adobe Photoshop 7.0 software (Adobe) to optimally visualize the expression patterns. Quantitative image analyses were processed using image-based morphometric analysis (NIS-Elements D3.1). Ten animals were quantified for each treatment.

Statistical analysis

All data are presented as mean \pm SEM. Statistical analysis and graphical representation of the data were performed using GraphPad Prism 5.0 (GraphPad Software). Statistical significance was performed using a Student's *t*-test, ANOVA, or χ^2 test as appropriate. Statistical significance is indicated by *, where $P < 0.05$, and ***, where $P < 0.0001$.

Supplementary material

Supplementary material is available at *Journal of Molecular Cell Biology* online.

Funding

This study was supported by grants from the National Natural Science Foundation of China (91331104), the 973 Program (2013CB835200, 2013CB835204), Bureau of Science and Technology of Yunnan Province (2015FA026), and the Youth Innovation Promotion Association, Chinese Academy of Sciences.

Conflict of interest: none declared.

References

- Ai, H., Fang, X., Yang, B., et al. (2015). Adaptation and possible ancient inter-species introgression in pigs identified by whole-genome sequencing. *Nat. Genet.* 47, 217–225.
- Akey, J.M., Zhang, G., Zhang, K., et al. (2002). Interrogating a high-density SNP map for signatures of natural selection. *Genome Res.* 12, 1805–1814.
- Alexander, D.H., Novembre, J., and Lange, K. (2009). Fast model-based estimation of ancestry in unrelated individuals. *Genome Res.* 19, 1655–1664.
- Axelsson, E., Ratnakumar, A., Arendt, M.L., et al. (2013). The genomic signature of dog domestication reveals adaptation to a starch-rich diet. *Nature* 495, 360–364.
- Bandelt, H.J., Forster, P., and Rohlf, A. (1999). Median-joining networks for inferring intraspecific phylogenies. *Mol. Biol. Evol.* 16, 37–48.
- Bolger, A.M., Lohse, M., and Usadel, B. (2014). Trimmomatic: a flexible trimmer for Illumina sequence data. *Bioinformatics* 30, 2114–2120.
- Brady, J.P., Garland, D.L., Green, D.E., et al. (2001). AlphaB-crystallin in lens development and muscle integrity: a gene knockout approach. *Invest. Ophthalmol. Vis. Sci.* 42, 2924–2934.
- Browning, S.R., and Browning, B.L. (2007). Rapid and accurate haplotype phasing and missing-data inference for whole-genome association studies by use of localized haplotype clustering. *Am. J. Hum. Genet.* 81, 1084–1097.
- Bruno, W.J., Socci, N.D., and Halpern, A.L. (2000). Weighted neighbor joining: a likelihood-based approach to distance-based phylogeny reconstruction. *Mol. Biol. Evol.* 17, 189–197.
- Carlborg, O., Hocking, P.M., Burt, D.W., et al. (2004). Simultaneous mapping of epistatic QTL in chickens reveals clusters of QTL pairs with similar genetic effects on growth. *Genet. Res.* 83, 197–209.
- Carlborg, O., Kerje, S., Schutz, K., et al. (2003). A global search reveals epistatic interaction between QTL for early growth in the chicken. *Genome Res.* 13, 413–421.
- Carneiro, M., Rubin, C.J., Di Palma, F., et al. (2014). Rabbit genome analysis reveals a polygenic basis for phenotypic change during domestication. *Science* 345, 1074–1079.
- Carroll, S.B. (2008). Evo-devo and an expanding evolutionary synthesis: a genetic theory of morphological evolution. *Cell* 134, 25–36.
- Chen, H., Shi, S., Acosta, L., et al. (2004). BMP10 is essential for maintaining cardiac growth during murine cardiogenesis. *Development* 131, 2219–2231.
- Chen, H., Yong, W., Ren, S., et al. (2006). Overexpression of bone morphogenetic protein 10 in myocardium disrupts cardiac postnatal hypertrophic growth. *J. Biol. Chem.* 281, 27481–27491.
- Danecek, P., Auton, A., Abecasis, G., et al. (2011). The variant call format and VCFtools. *Bioinformatics* 27, 2156–2158.
- Darwin, C. (1868) *The Variation of Animals and Plants Under Domestication* London, UK: John Murray.
- de Celis, J.F., and Barrio, R. (2008). Regulation and function of Spalt proteins during animal development. *Int. J. Dev. Biol.* 53, 1385–1398.
- Devlin, R.H., Sakhrani, D., Tymchuk, W.E., et al. (2009). Domestication and growth hormone transgenesis cause similar changes in gene expression in coho salmon (*Oncorhynchus kisutch*). *Proc. Natl Acad. Sci. USA* 106, 3047–3052.
- Elferink, M.G., Megens, H.J., Vereijken, A., et al. (2012). Signatures of selection in the genomes of commercial and non-commercial chicken breeds. *PLoS One* 7, e32720.
- Eriksson, J., Larson, G., Gunnarsson, U., et al. (2008). Identification of the yellow skin gene reveals a hybrid origin of the domestic chicken. *PLoS Genet.* 4, e1000010.
- Fan, W.L., Ng, C.S., Chen, C.F., et al. (2013). Genome-wide patterns of genetic variation in two domestic chickens. *Genome Biol. Evol.* 5, 1376–1392.
- Folkman, J., and Shing, Y. (1992). Angiogenesis. *J. Biol. Chem.* 267, 10931–10934.
- Gou, X., Wang, Z., Li, N., et al. (2014). Whole genome sequencing of six dog breeds from continuous altitudes reveals adaptation to high-altitude hypoxia. *Genome Res.* 24, 1308–1315.
- Gu, X., Feng, C., Ma, L., et al. (2011). Genome-wide association study of body weight in chicken F2 resource population. *PLoS One* 6, e21872.
- Gudbjartsson, D.F., Walters, G.B., Thorleifsson, G., et al. (2008). Many sequence variants affecting diversity of adult human height. *Nat. Genet.* 40, 609–615.
- Kamberov, Y.G., Wang, S., Tan, J., et al. (2013). Modeling recent human evolution in mice by expression of a selected EDAR variant. *Cell* 152, 691–702.
- Kawakami, Y., Uchiyama, Y., Rodriguez Esteban, C., et al. (2009). Sall genes regulate region-specific morphogenesis in the mouse limb by modulating Hox activities. *Development* 136, 585–594.
- Kim, D., Langmead, B., and Salzberg, S.L. (2015). HISAT: a fast spliced aligner with low memory requirements. *Nat. Methods* 12, 357–360.
- Kim, O., Yoon, J.H., Choi, W.S., et al. (2014). GKN2 contributes to the homeostasis of gastric mucosa by inhibiting GKN1 activity. *J. Cell. Physiol.* 229, 762–771.
- Kimmel, C.B., Ballard, W.W., Kimmel, S.R., et al. (1995). Stages of embryonic development of the zebrafish. *Dev. Dyn.* 203, 253–310.
- Kivimae, S., Martin, P.M., Kapfhamer, D., et al. (2011). Abnormal behavior in mice mutant for the Disc1 binding partner, Dixdc1. *Transl. Psychiatry* 1, e43.
- Kohno, D., Lee, S., Harper, M.J., et al. (2014). Dnmt3a in Sim1 neurons is necessary for normal energy homeostasis. *J. Neurosci.* 34, 15288–15296.

- Kojima, T., Asano, S., and Takahashi, N. (2013). Teratogenic factors affect transcription factor expression. *Biosci. Biotechnol. Biochem.* *77*, 1035–1041.
- Kong, Y. (2011). Btrim: a fast, lightweight adapter and quality trimming program for next-generation sequencing technologies. *Genomics* *98*, 152–153.
- Lamichhaney, S., Berglund, J., Almen, M.S., et al. (2015). Evolution of Darwin's finches and their beaks revealed by genome sequencing. *Nature* *518*, 371–375.
- Lango Allen, H., Estrada, K., Lettre, G., et al. (2015). Hundreds of variants clustered in genomic loci and biological pathways affect human height. *Nature* *467*, 832–838.
- Lawler, A. (2014) *Why did the Chicken Cross the World?: The Epic Saga of the Bird that Powers Civilization*. New York: Atria Books.
- Lawson, D.J., Hellenthal, G., Myers, S., et al. (2012). Inference of population structure using dense haplotype data. *PLoS Genet.* *8*, e1002453.
- Lawson, N.D., and Weinstein, B.M. (2002). In vivo imaging of embryonic vascular development using transgenic zebrafish. *Dev. Biol.* *248*, 307–318.
- Locke, A.E., Kahali, B., Berndt, S.I., et al. (2015). Genetic studies of body mass index yield new insights for obesity biology. *Nature* *518*, 197–206.
- Makvandi-Nejad, S., Hoffman, G.E., Allen, J.J., et al. (2012). Four loci explain 83% of size variation in the horse. *PLoS One* *7*, e39929.
- McKenna, A., Hanna, M., Banks, E., et al. (2010). The Genome Analysis Toolkit: a MapReduce framework for analyzing next-generation DNA sequencing data. *Genome Res.* *20*, 1297–1303.
- Menheniott, T.R., Kurklu, B., and Giraud, A.S. (2013). Gastrophilins: stomach-specific proteins with putative homeostatic and tumor suppressor roles. *Am. J. Physiol. Gastrointest. Liver Physiol.* *304*, G109–G121.
- Miao, Y.W., Peng, M.S., Wu, G.S., et al. (2013). Chicken domestication: an updated perspective based on mitochondrial genomes. *Heredity* *110*, 277–282.
- Neuhaus, H., Rosen, V., and Thies, R.S. (1999). Heart specific expression of mouse BMP-10 a novel member of the TGF-beta superfamily. *Mech. Dev.* *80*, 181–184.
- Ousman, S.S., Tomooka, B.H., van Noort, J.M., et al. (2007). Protective and therapeutic role for alphaB-crystallin in autoimmune demyelination. *Nature* *448*, 474–479.
- Parrish, M., Ott, T., Lance-Jones, C., et al. (2004). Loss of the Sall3 gene leads to palate deficiency, abnormalities in cranial nerves, and perinatal lethality. *Mol. Cell. Biol.* *24*, 7102–7112.
- Pashmforoush, M., Lu, J.T., Chen, H., et al. (2004). Nkx2-5 pathways and congenital heart disease; loss of ventricular myocyte lineage specification leads to progressive cardiomyopathy and complete heart block. *Cell* *117*, 373–386.
- Perteau, M., Perteau, G.M., Antonescu, C.M., et al. (2015). StringTie enables improved reconstruction of a transcriptome from RNA-seq reads. *Nat. Biotechnol.* *33*, 290–295.
- Purcell, S., Neale, B., Todd-Brown, K., et al. (2007). PLINK: a tool set for whole-genome association and population-based linkage analyses. *Am. J. Hum. Genet.* *81*, 559–575.
- Qanbari, S., Pausch, H., Jansen, S., et al. (2014). Classic selective sweeps revealed by massive sequencing in cattle. *PLoS Genet.* *10*, e1004148.
- Reimand, J., Arak, T., and Vilo, J. (2011). g:Profiler—a web server for functional interpretation of gene lists (2011 update). *Nucleic Acids Res.* *39*, W307–315.
- Rimbault, M., Beale, H.C., Schoenebeck, J.J., et al. (2013). Derived variants at six genes explain nearly half of size reduction in dog breeds. *Genome Res.* *23*, 1985–1995.
- Roots, C. (2007) *Domestication*. Westport: Greenwood Press.
- Rubin, C.J., Megens, H.J., Martinez Barrio, A., et al. (2012). Strong signatures of selection in the domestic pig genome. *Proc. Natl Acad. Sci. USA* *109*, 19529–19536.
- Rubin, C.J., Zody, M.C., Eriksson, J., et al. (2010). Whole-genome resequencing reveals loci under selection during chicken domestication. *Nature* *464*, 587–591.
- Sewalem, A., Morrice, D.M., Law, A., et al. (2002). Mapping of quantitative trait loci for body weight at three, six, and nine weeks of age in a broiler layer cross. *Poult. Sci.* *81*, 1775–1781.
- Shapiro, M.D., Kronenberg, Z., Li, C., et al. (2013). Genomic diversity and evolution of the head crest in the rock pigeon. *Science* *339*, 1063–1067.
- Shikachi, Y., Saiura, A., Kubo, T., et al. (2009). SALL3 interacts with DNMT3A and shows the ability to inhibit CpG island methylation in hepatocellular carcinoma. *Mol. Biol. Cell* *29*, 1944–1958.
- Shriver, M.D., Kennedy, G.C., Parra, E.J., et al. (2004). The genomic distribution of population substructure in four populations using 8525 autosomal SNPs. *Hum. Genomics* *1*, 274–286.
- Siwek, M., Cornelissen, S.J., Buitenhuis, A.J., et al. (2004). Quantitative trait loci for body weight in layers differ from quantitative trait loci specific for antibody responses to sheep red blood cells. *Poult. Sci.* *83*, 853–859.
- Stephens, M., and Donnelly, P. (2003). A comparison of bayesian methods for haplotype reconstruction from population genotype data. *Am. J. Hum. Genet.* *73*, 1162–1169.
- Sutter, N.B., Bustamante, C.D., Chase, K., et al. (2007). A single IGF1 allele is a major determinant of small size in dogs. *Science* *316*, 112–115.
- Tamura, K., Peterson, D., Peterson, N., et al. (2011). MEGA5: molecular evolutionary genetics analysis using maximum likelihood, evolutionary distance, and maximum parsimony methods. *Mol. Biol. Evol.* *28*, 2731–2739.
- Tercic, D., Holcman, A., Dovc, P., et al. (2009). Identification of chromosomal regions associated with growth and carcass traits in an F(3) full sib intercross line originating from a cross of chicken lines divergently selected on body weight. *Anim. Genet.* *40*, 743–748.
- Trapnell, C., Roberts, A., Goff, L., et al. (2012). Differential gene and transcript expression analysis of RNA-seq experiments with TopHat and Cufflinks. *Nat. Protoc.* *7*, 562–578.
- Wang, K., Li, M., and Hakonarson, H. (2010). ANNOVAR: functional annotation of genetic variants from high-throughput sequencing data. *Nucleic Acids Res.* *38*, e164.
- Wang, M.S., Li, Y., Peng, M.S., et al. (2015a). Genomic analyses reveal potential independent adaptation to high altitude in Tibetan chickens. *Mol. Biol. Evol.* *32*, 1880–1889.
- Wang, M.S., Zhang, R.W., Su, L.Y., et al. (2016). Positive selection rather than relaxation of functional constraint drives the evolution of vision during chicken domestication. *Cell Res.* *26*, 556–573.
- Wang, W.H., Wang, J.Y., Zhang, T., et al. (2015b). Genome-wide association study of growth traits in Jinghai Yellow chicken hens using SLAF-seq technology. *Anim. Genet.* doi:10.1111/age.12346.
- Westerfield, M. (1993) *The Zebrafish Book: A Guide for the Laboratory Use of Zebrafish*. Eugene: The University of Oregon Press.
- Xie, L., Luo, C., Zhang, C., et al. (2012). Genome-wide association study identified a narrow chromosome 1 region associated with chicken growth traits. *PLoS One* *7*, e30910.
- Yang, J., Lee, S.H., Goddard, M.E., et al. (2011). GCTA: a tool for genome-wide complex trait analysis. *Am. J. Hum. Genet.* *88*, 76–82.
- Yang, X., Zhang, Z., Qiu, M., et al. (2013). Glypican-5 is a novel metastasis suppressor gene in non-small cell lung cancer. *Cancer Lett.* *341*, 265–273.
- Yi, G., Qu, L., Liu, J., et al. (2014). Genome-wide patterns of copy number variation in the diversified chicken genomes using next-generation sequencing. *BMC Genomics* *15*, 962.
- Yoon, J.H., Choi, W.S., Kim, O., et al. (2014). The role of gastrophilin 1 in gastric cancer. *J. Gastric Cancer* *14*, 147–155.
- Young, R.S., Hayashizaki, Y., Andersson, R., et al. (2015). The frequent evolutionary birth and death of functional promoters in mouse and human. *Genome Res.* *25*, 1546–1557.

Figure S1: Yuanbao chicken (middle) and indigenous chicken (right and left)



Figure S2: Genome sequence depth for each bird in this study. DWS, Daweishan chicken; RJF, Red Junglefowl; YB, Yuanbao chicken.

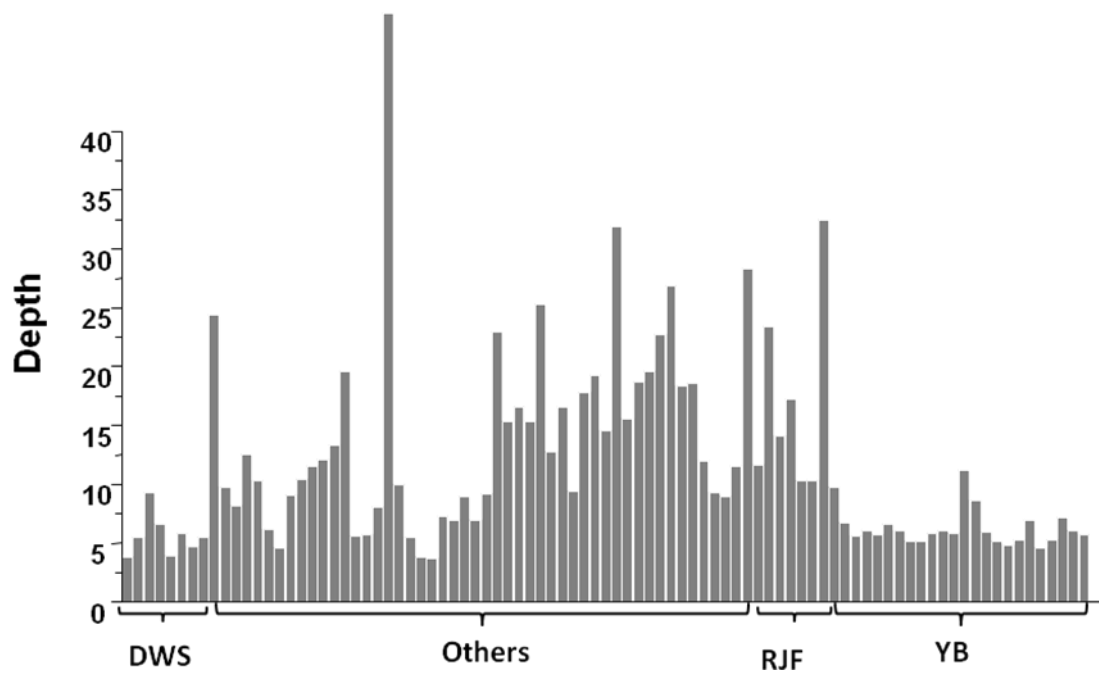


Figure S3: Nucleotide diversity for each chicken group. DWS, Daweishan chicken; RJF, Red Junglefowl; YB, Yuanbao chicken.

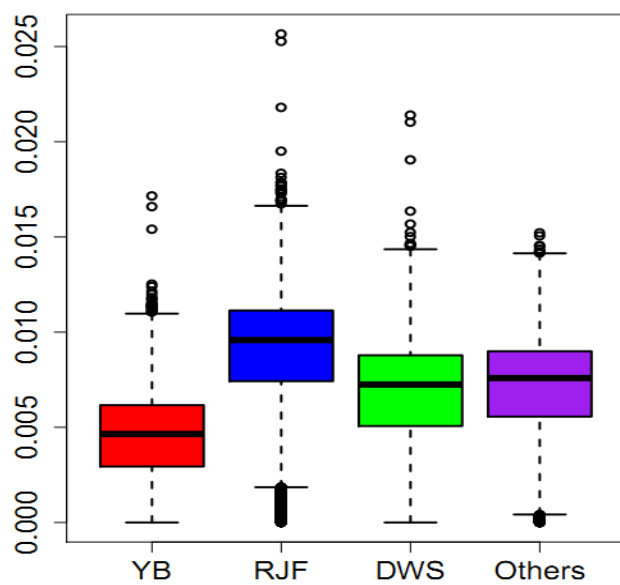


Figure S4: Population structure inferred by ADMIXTURE. K=2 is the best.

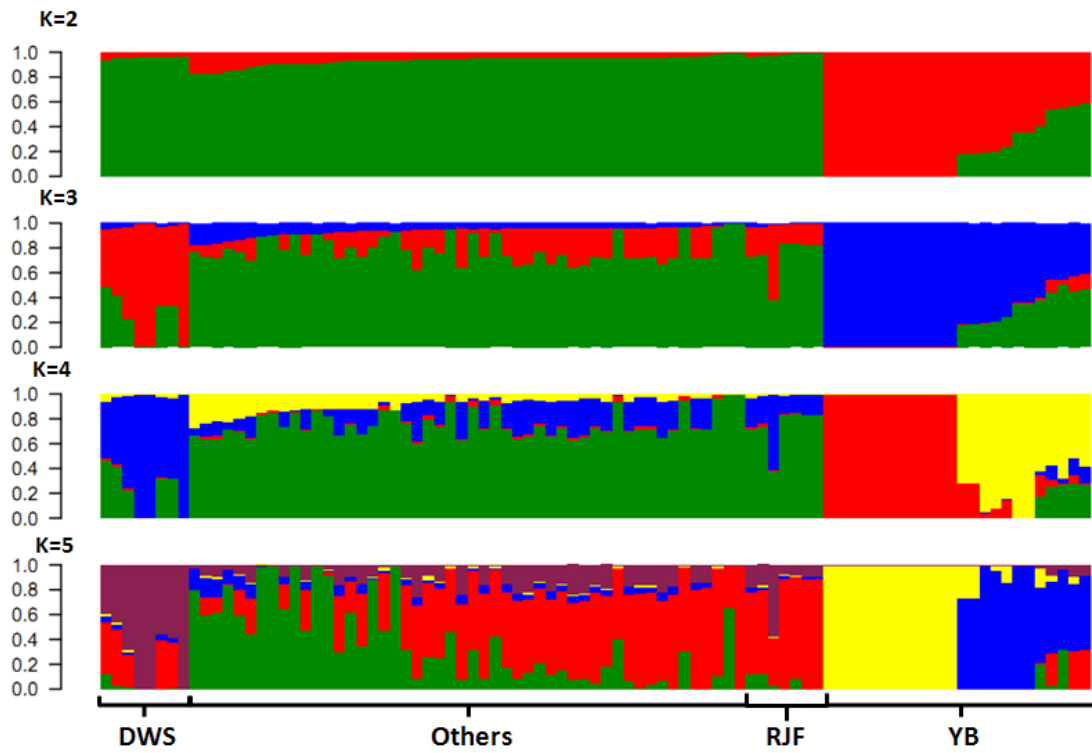


Figure S5: Population structure inferred by ChromoPainter and fineSTRUCTURE.

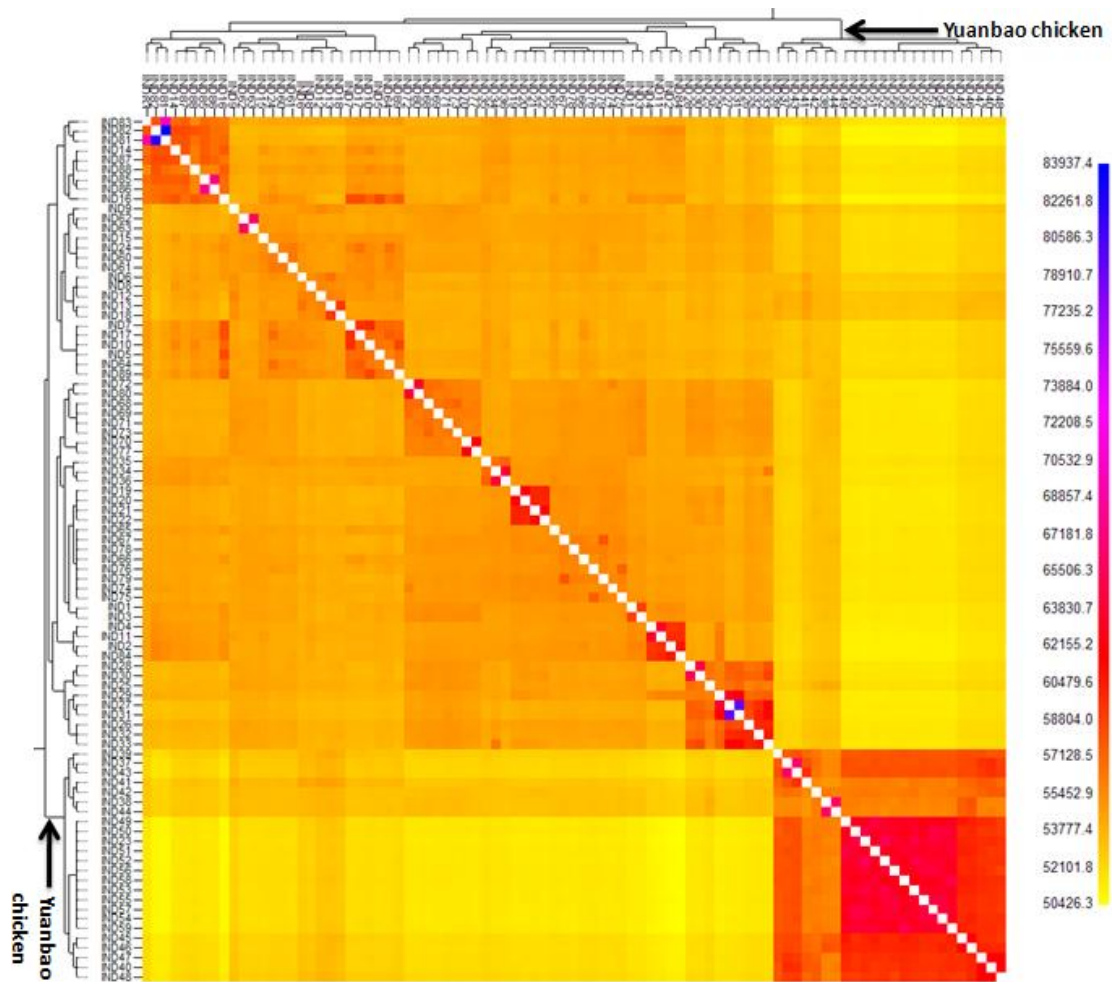


Figure S6: Expression of GKN1(A) and GKN1(B) in Red junglefowl (RJF), Yuanbao chicken (YB) and village domestic chicken (VC)

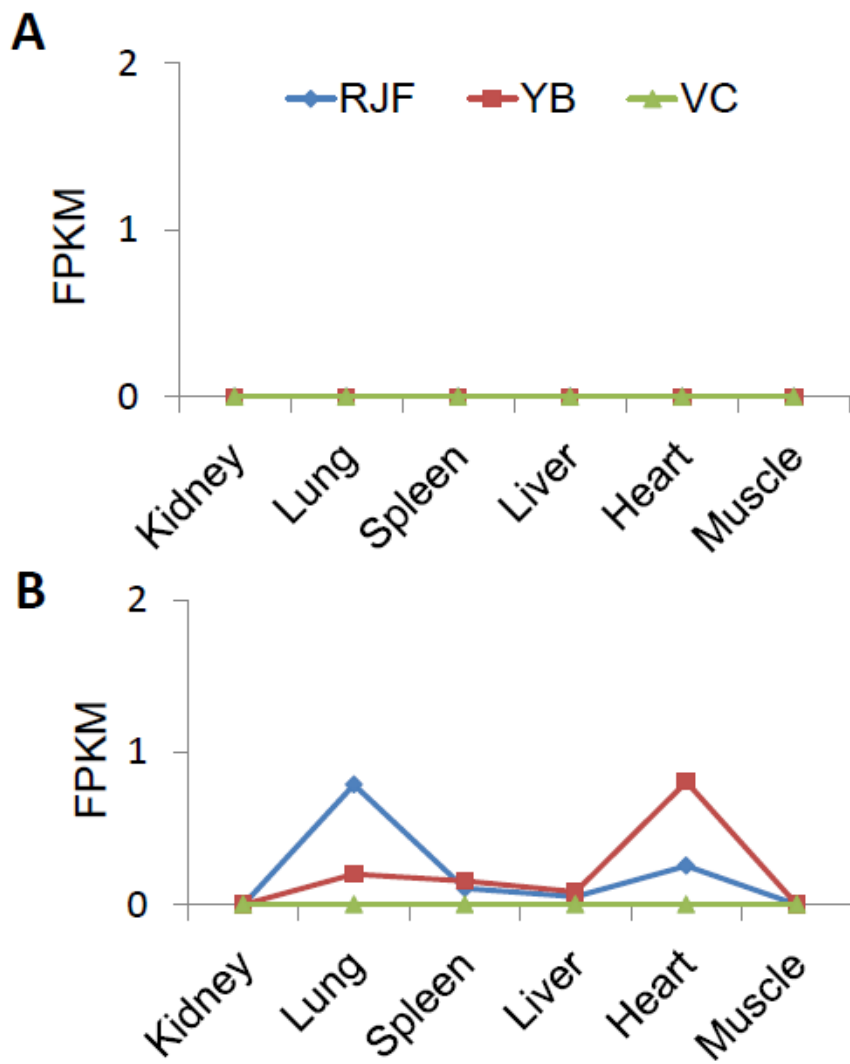


Figure S7: RT-PCR for *BMP10* with template generated from the brain, kidney, lung, spleen, liver, heart and muscle tissue of the chicken.

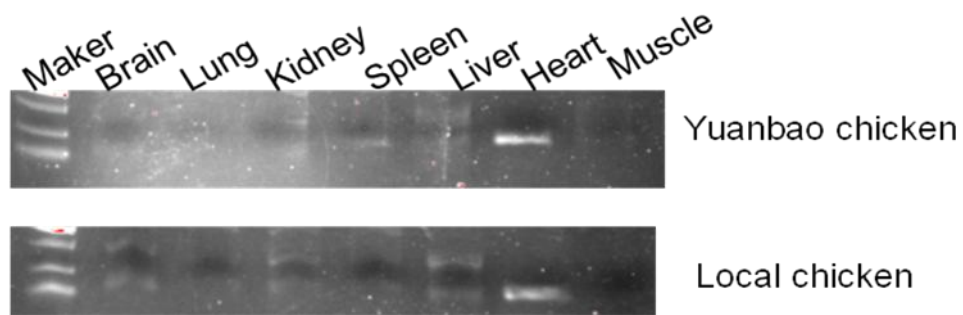


Figure S8: 21 SNPs functionally examined by the electrophoretic mobility shift assay (EMSA) based on 20 probes. “+” and “-” refer to probes with the Yuanbao chicken mutated allele and reference alleles, respectively. 1, 2, 3 refer to EMSA performed in 3 different indigenous chickens, individually, and 4 refer to the EMSA performed in the Yuanbao chicken.

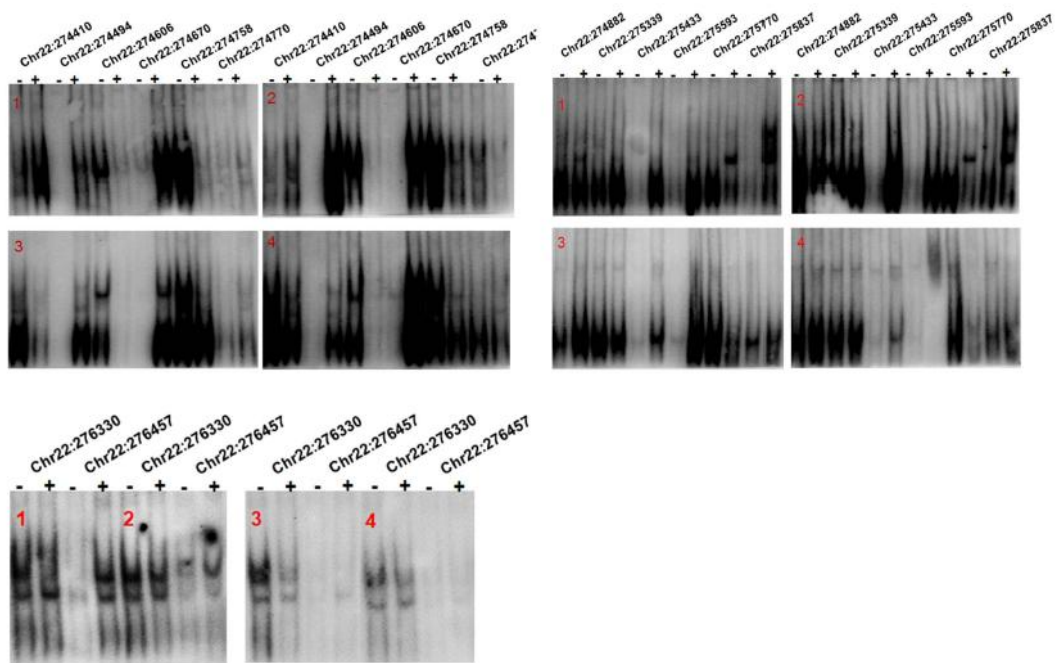


Figure S9: Wild-type zebrafish *BMP10* overexpression causes a decrease in the body length and curved body axis in the zebrafish

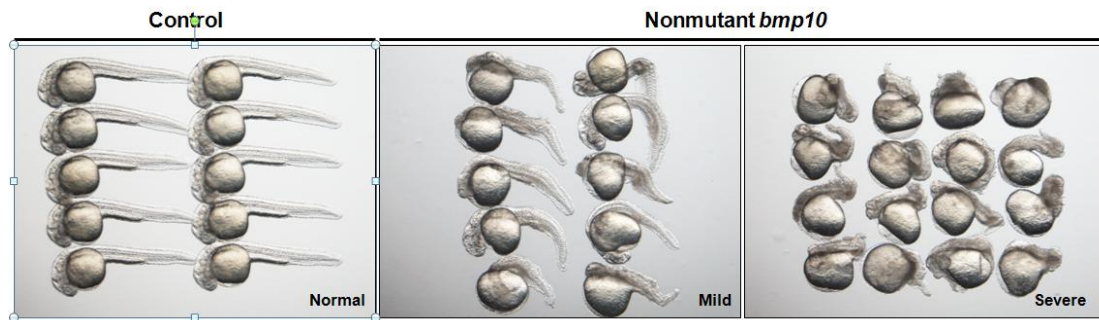


Figure S10: Wild-type *bmp10* overexpression inhibits angiogenic vessel growth in the zebrafish. Each column shows five examples of the phenotype induced in trunk angiogenesis

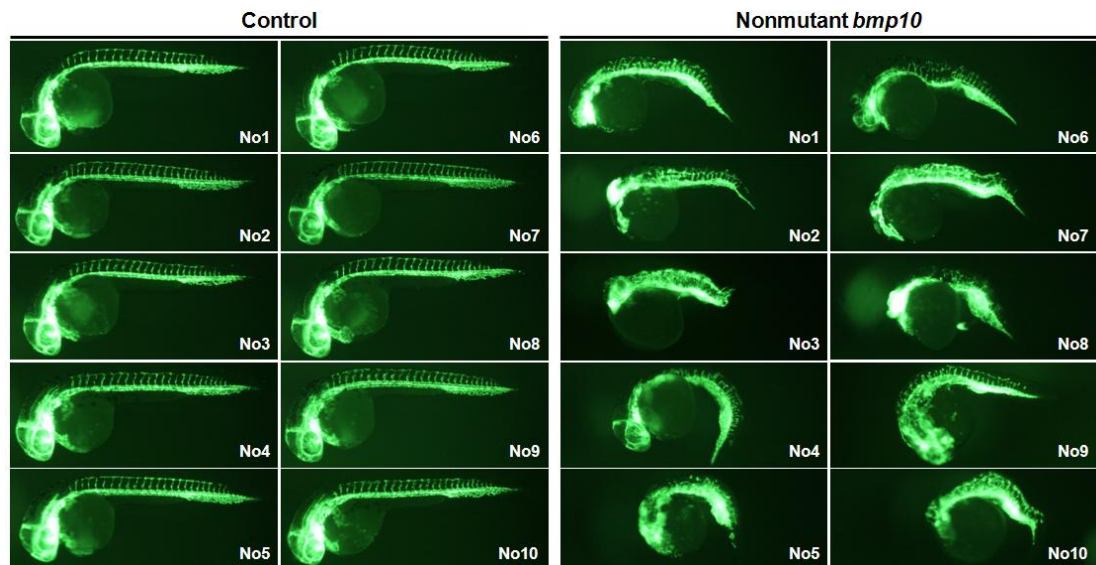


Figure S11: Expression of GPC5(A) and SALL3(B) in Red junglefowl(RJF), Yuanbao chicken(YB) and village domestic chicken(VC)

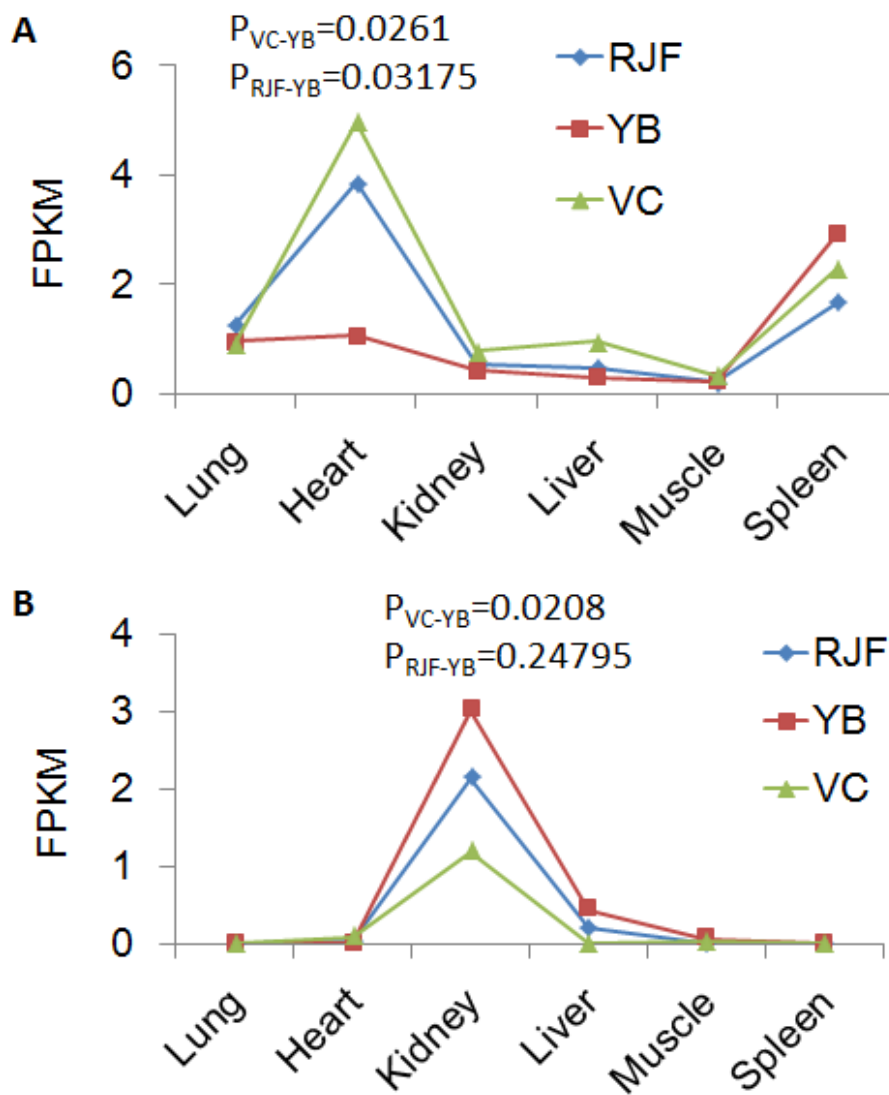


Figure S12: Expression of 13 genes in Red junglefowl(RJF), Yuanbao chicken(YB) and village domestic chicken(VC)

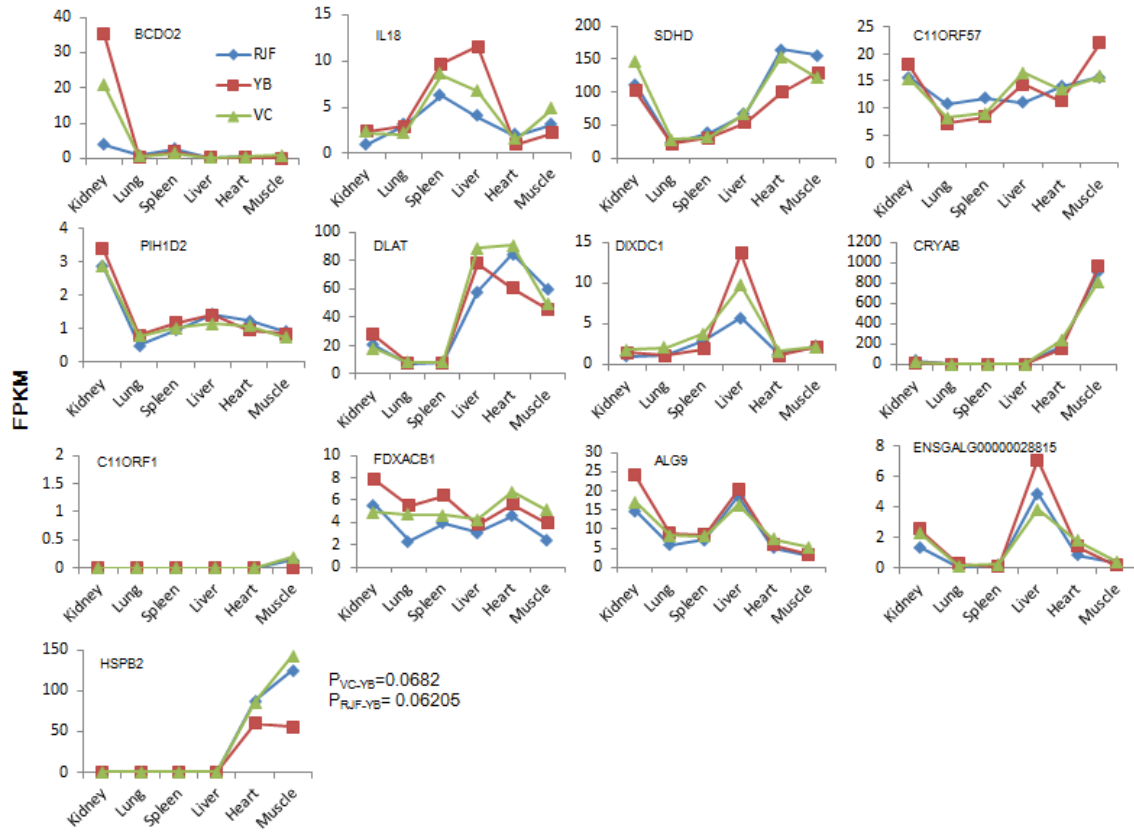


Table S1: Sample information for each bird used in this study. The shaded individuals were sequenced in this study. In total, 42 birds were used to perform whole genome resequencing.

Group ID	Sample ID	Information	Group ID	Sample ID	Information
DWS	Ypt566	Daweishan, Yunnan, China	Others	Game fowl4	PRJNA241474
DWS	Ypt567	Daweishan, Yunnan, China	Others	Game fowl5	PRJNA241474
DWS	Ypt568	Daweishan, Yunnan, China	Others	Game fowl6	PRJNA241474
DWS	Ypt569	Daweishan, Yunnan, China	Others	Game fowl7	PRJNA241474
DWS	Ypt571	Daweishan, Yunnan, China	Others	Game fowl8	PRJNA241474
DWS	Ypt572	Daweishan, Yunnan, China	Others	Tibet chciken5	PRJNA241474
DWS	Ypt573	Daweishan, Yunnan, China	Others	Tibet chciken6	PRJNA241474
DWS	Ypt574	Daweishan, Yunnan, China	Others	Tibet chciken7	PRJNA241474
Others	L2	SRP022583	Others	Tibet chciken8	PRJNA241474
Others	SAMN02486156	SRP034930	Others	Tibet chciken9	PRJNA241474
Others	SAMN02486157	SRP034930	Others	Tibet chciken10	PRJNA241474
Others	SAMN02486158	SRP034930	Others	Tibet chciken11	PRJNA241474
Others	SAMN02486159	SRP034930	Others	production	PRJNA241474
Others	SAMN02486160	SRP034930	RJF	Red Junglefowl1	PRJNA241474
Others	SAMN02486162	SRP034930	RJF	Red Junglefowl2	PRJNA241474
Others	SAMN02486163	SRP034930	RJF	Red Junglefowl3	PRJNA241474
Others	SAMN02486164	SRP034930	RJF	Red Junglefowl4	PRJNA241474
Others	SAMN02486165	SRP034930	RJF	SAMN02486161	SRP034930
Others	SAMN02486166	SRP034930	RJF	Ypt570	Daweishan, Yunnan, China
Others	SAMN02486167	SRP034930	RJF	Red Junglefowl5	PRJNA241474
Others	Silkia	SRP022583	YB	Ypt601	Jijing, Shandong, China
Others	Tibet chciken1	PRJNA241474	YB	Ypt578	Xuzhou, Jiangsu, China
Others	Tibet chciken2	PRJNA241474	YB	Ypt579	Xuzhou, Jiangsu, China
Others	Tibet chciken3	PRJNA241474	YB	Ypt580	Xuzhou, Jiangsu, China
Others	Tibet chciken4	PRJNA241474	YB	Ypt581	Xuzhou, Jiangsu, China
Others	Ypt648	GuanZhou, China	YB	Ypt582	Xuzhou, Jiangsu, China
Others	Ypt575	PanZhihua, Yunnan, China	YB	Ypt583	Xuzhou, Jiangsu, China
Others	Ypt576	PanZhihua, Yunnan, China	YB	Ypt584	Xuzhou, Jiangsu, China
Others	Ypt577	PanZhihua, Yunnan, China	YB	Ypt585	Xuzhou, Jiangsu, China
Others	Ypt642	GuanZhou, China	YB	Ypt586	Xuzhou, Jiangsu, China
Others	Ypt643	GuanZhou, China	YB	Ypt587	Xuzhou, Jiangsu, China
Others	Ypt645	GuanZhou, China	YB	Ypt588	Xuzhou, Jiangsu, China
Others	Ypt646	GuanZhou, China	YB	Ypt589	Xuzhou, Jiangsu, China
Others	Ypt647	GuanZhou, China	YB	Ypt590	Jijing, Shandong, China
Others	Native chicken1	PRJNA241474	YB	Ypt591	Jijing, Shandong, China
Others	Native chicken2	PRJNA241474	YB	Ypt592	Jijing, Shandong, China
Others	Native chicken3	PRJNA241474	YB	Ypt593	Jijing, Shandong, China
Others	Native chicken4	PRJNA241474	YB	Ypt594	Jijing, Shandong, China

Others	Native chicken5	PRJNA241474	YB	Ypt595	Jijing,Shandong, China
Others	Native chicken6	PRJNA241474	YB	Ypt596	Jijing,Shandong, China
Others	Native chicken7	PRJNA241474	YB	Ypt597	Jijing,Shandong, China
Others	Native chicken8	PRJNA241474	YB	Ypt598	Jijing,Shandong, China
Others	Game fowl1	PRJNA241474	YB	Ypt599	Jijing,Shandong, China
Others	Game fowl2	PRJNA241474	YB	Ypt600	Jijing,Shandong, China
Others	Game fowl3	PRJNA241474			

Table S2: Distribution of SNPs in the chicken population

Terms	Number	Proportion
exonic	329569	1.55%
intronic	9074575	42.63%
intergenic	11033477	51.83%
UTRs	271784	1.28%
others	576907	2.71%
Total	21286312	100.00%

Table S3: Distribution of SNPs located in protein coding regions in the chicken population

Terms	Synonymous	Nonsynonymous	Stop gain	Stop loss
Number of SNV	226713	101999	739	73
Number of genes	13985	12601	633	71
Number of transcripts	563	13290	649	71

Table S4: Functional enrichment of genes identified by F_{ST}

P-value	Gene number	ID	Term	Description
4.42E-02	3	GO:0034116	BP	positive regulation of heterotypic cell-cell adhesion
2.56E-02	3	GO:0005577	CC	fibrinogen complex
5.00E-02	8	GO:0050839	MF	cell adhesion molecule binding
3.46E-02	4	GO:0008484	MF	sulfuric ester hydrolase activity
1.60E-03	3	HP:0012223	hp	Splenic rupture
5.00E-02	4	HP:0010990	hp	Abnormality of the common coagulation pathway
1.12E-03	4	HP:0011898	hp	Abnormality of circulating fibrinogen
1.12E-03	4	HP:0011900	hp	Hypofibrinogenemia
1.72E-02	12	HP:0010985	hp	Gonosomal inheritance
1.52E-02	12	HP:0001417	hp	X-linked inheritance
1.36E-03	10	HP:0001419	hp	X-linked recessive inheritance
6.30E-03	3	HP:0000420	hp	Short nasal septum
5.00E-02	6	KEGG:04514	ke	Cell adhesion molecules (CAMs)

Table S5: Functional enrichment of genes identified by LSBL

P-value	Gene number	ID	Term	Description
3.59E-02	3	GO:0034116	BP	positive regulation of heterotypic cell-cell adhesion
2.08E-02	3	GO:0005577	CC	fibrinogen complex
5.00E-02	6	GO:0008170	MF	N-methyltransferase activity
5.00E-02	6	HP:0003256	hp	Abnormality of the coagulation cascade
3.52E-03	5	HP:0010990	hp	Abnormality of the common coagulation pathway
1.50E-03	4	HP:0011898	hp	Abnormality of circulating fibrinogen
1.50E-03	4	HP:0011900	hp	Hypofibrinogenemia
8.01E-03	3	HP:0000420	hp	Short nasal septum
2.04E-03	3	HP:0012223	hp	Splenic rupture
1.44E-02	9	HP:0001419	hp	X-linked recessive inheritance
1.85E-02	5	KEGG:04514	ke	Cell adhesion molecules (CAMs)
5.00E-02	2	KEGG:00020	ke	Citrate cycle (TCA cycle)
4.61E-02	2	KEGG:00062	ke	Fatty acid elongation

Table S6: Genes located in chr24: 6.17Mb-6.25Mb

Ensembl Gene ID	Name	Descriptions	Biological function	References
ENSGALG00000007868	BCDO2	beta-carotene oxygenase 2	body skin color	(1)
ENSGALG00000007874	IL18	Gallus gallus interleukin 18	immune responses	(2)
ENSGALG00000007878	SDHD	succinate dehydrogenase	energy conversion	(3)
ENSGALG00000007882	C11orf57	chromosome 11 open reading frame 57	Not available	
ENSGALG00000007885	PIH1D2	PIH1 domain containing 2	Ral GTPase binding	http://www.genecards.org/
ENSGALG00000007904	DLAT	dihydrolipoamide S-acetyltransferase	energy conversion	http://www.genecards.org/
ENSGALG00000007929	DIXDC1	DIX domain containing 1	major mental illnesses	(4)
ENSGALG00000007945	CRYAB	Alpha-crystallin B chain	in both the immune system and central nervous system (CNS)	(5)
ENSGALG00000007950	C11orf1	chromosome 11 open reading frame 1	Not available	Not available
ENSGALG00000007967	FDXACB1	ferredoxin-fold anticodon binding domain containing 1	magnesium ion binding and phenylalanine-tRNA ligase activity	http://www.genecards.org/
ENSGALG00000021174	NA	Not available	Not available	Not available
ENSGALG00000028815	NA	Not available	Not available	Not available
ENSGALG00000028966	HSPB2	heat shock protein beta-2	maintain muscle cell integrity in some skeletal muscles	(6)

1. Eriksson J, *et al.* (2008) Identification of the yellow skin gene reveals a hybrid origin of the domestic chicken. *PLoS genetics* 4(2):e1000010.
2. Gobel TW, *et al.* (2003) IL-18 stimulates the proliferation and IFN-gamma release of CD4+ T cells in the chicken: conservation of a Th1-like system in a nonmammalian species. *Journal of immunology (Baltimore, Md. : 1950)* 171(4):1809-1815.
3. Alston CL, *et al.* (2015) A recessive homozygous p.Asp92Gly SDHD mutation causes prenatal cardiomyopathy and a severe mitochondrial complex II deficiency.

Human genetics 134(8):869-879.

4. Kivimae S, *et al.* (2011) Abnormal behavior in mice mutant for the Disc1 binding partner, Dixdc1. *Translational psychiatry* 1:e43.
5. Ousman SS, *et al.* (2007) Protective and therapeutic role for alphaB-crystallin in autoimmune demyelination. *Nature* 448(7152):474-479.
6. Brady JP, *et al.* (2001) AlphaB-crystallin in lens development and muscle integrity: a gene knockout approach. *Investigative ophthalmology & visual science* 42(12):2924-2934.

Table S7: Primers used for the amplification and sequencing of the upstream and first exon region of *BMP10* in the chicken

Primer ID	Sequence	Annealing temperature
cBMP10-1F	5' GAAGGAAAGCCAAACTCAC 3'	63°C
cBMP10-1R	5' CAGACAAGCACGGATAACA 3'	
cBMP10-2F	5' TTCAGCCCTAACCTCGTA 3'	60°C
cBMP10-2R	5' TCTTCTATGGTCGCCTTGC 3'	
cBMP10-3F	5' ATAAGAGAGGCAAGGCGAC 3'	60°C
cBMP10-3R	5' TTGTCTGTTGCTAATGGTGC 3'	
cBMP10-4F	5' GGAGGCAGAAAGAAAGAGC 3'	67°C
cBMP10-4R	5' GGTGAACCAAGAGGCAGAG 3'	
cBMP10-5F	5' TCAGCCCTAACCTCGTA 3'	50°C
cBMP10-5R	5' CAGCCTTATCAAAGACTCATC 3'	
cBMP10-5F	5' TCAGCCCTAACCTCGTA 3'	58°C
cBMP10-5R-1	5' CGTTCCTCCTTCACAGATA 3'	
cBMP10-6F	5' CTATGCTTAGCCACAATG 3'	60°C
cBMP10-6R	5' AAAGCCAGGTCTCAGTAA 3'	
Sequencing primers		
cBMP10-1-A	5' GGCACAGTGATGATGGGTT 3'	
cBMP10-1-B	5' AGCCCAACCTCTGCTACAA 3'	
cBMP10-2-A	5' TAGAGGCTCCATAGGATTTACG 3'	
cBMP10-2-A	5' TCCTATGGAGCCTCTACTGAA 3'	
cBMP10-3-A	5' TGTGCTCAGTGCCTGGTTG 3'	
cBMP10-3-B	5' GTGGCAAGGTGAACCAAGAG 3'	

Table S8: Primer used for qPCR for *BMP10*

Primer ID	Sequence	Annealing temperature
cBMP10-1F	5' CTGGACTTGGAGAACCTG 3'	56°C
cBMP10-1R	5' AGGAATCCCAGCCAATCT 3'	

Table S9: RNA-seq information data used in analyses

SampleID	Tissue	Group	Total of Pair-end reads	Mapping rate(%)
s570F_HNGYWCCXX_L4	Lung	RJF	28264090	75.25
s540F_HNGYWCCXX_L4	Lung	RJF	21528202	65.07
s2827F_HNGYWCCXX_L4	Lung	RJF	21630178	77.4
s592F_HNGYWCCXX_L5	Lung	YB	22423302	83.75
s583F_HNGYWCCXX_L4	Lung	YB	22472666	82.79
s530F_HNGYWCCXX_L8	Lung	VC	22277524	74.1
s529F_HNGYWCCXX_L4	Lung	VC	19136029	56.37
s525F_HNGYWCCXX_L7	Lung	VC	22405300	75.22
s2828H_HNGYWCCXX_L5	Heart	RJF	19751609	83.77
s570H_HNGYWCCXX_L8	Heart	RJF	23332135	84.81
s540H_HNGYWCCXX_L4	Heart	RJF	29066831	83.63
s592H_HNG5YCCXX_L3	Heart	YB	32305393	83.81
s583H_HNGYWCCXX_L7	Heart	YB	23191090	84.5
s530H_HNGYWCCXX_L7	Heart	VC	20429389	83.26
s525H_HNGYWCCXX_L7	Heart	VC	17372973	83.66
s2828K_HNGYWCCXX_L8	Kidney	RJF	25997646	80.64
s570K_HNGYWCCXX_L3	Kidney	RJF	25870169	81.26
s540K_HNGYWCCXX_L7	Kidney	RJF	27158204	81.77
s2827K_HNGYWCCXX_L4	Kidney	RJF	24732370	81.58
s592K_HNGYWCCXX_L4	Kidney	YB	22512141	84.2
s583K_HNGYWCCXX_L5	Kidney	YB	20448738	82.07
s530K_HNGYWCCXX_L8	Kidney	VC	25898980	79.89
s525K_HNGYWCCXX_L7	Kidney	VC	22927844	78.84
s2828L_HNGYWCCXX_L8	Liver	RJF	25883409	83.5
s570L_HNGYWCCXX_L8	Liver	RJF	25831731	85.77
s540L_HNGYWCCXX_L4	Liver	RJF	21671206	83.85
s2827L_HNGYWCCXX_L3	Liver	RJF	21462140	85.81
s592L_HNGYWCCXX_L7	Liver	YB	24955899	86.01
s583L_HNGYWCCXX_L7	Liver	YB	23851464	84.97
s530L_HNGYWCCXX_L4	Liver	VC	20425602	85.98
s525L_HNGYWCCXX_L5	Liver	VC	23938249	81.17
s2828M_HNGYWCCXX_L7	Muscle	RJF	22635066	77.86
s570M_HNG3LCCXX_L2	Muscle	RJF	24689894	76.49
s540M_HNGYWCCXX_L4	Muscle	RJF	23304742	75.28
s2827M_HNH7JCCXX_L4	Muscle	RJF	28103332	72.31
s592M_HNGYWCCXX_L6	Muscle	YB	24681180	84.32
s583M_HNGYWCCXX_L5	Muscle	YB	23910975	75.63
s530M_HNGYWCCXX_L7	Muscle	VC	29503807	82.32
s525M_HNGYWCCXX_L8	Muscle	VC	27090438	71.04
s2828S_HNG5YCCXX_L3	Spleen	RJF	31176122	75.18

s570S_HNG3LCCXX_L2	Spleen	RJF	29053337	68.48
s540S_HNGYWCCXX_L3	Spleen	RJF	26980458	72.31
s2827S_HNGYWCCXX_L8	Spleen	RJF	23147032	77.33
s592S_HNGYWCCXX_L5	Spleen	YB	25051665	78.87
s583S_HNGYWCCXX_L7	Spleen	YB	22397054	82.03
s530S_HNGYWCCXX_L4	Spleen	VC	24655946	80.2
s525S_HNGYWCCXX_L6	Spleen	VC	21166277	80.95

Notes: Red junglefowl,RJF; Yuanbao chicken (YB) and village domestic chicken (VC)